

Control strategies for large-scale structural systems: high-rise buildings and multi-building systems

Francisco Palacios-Quiñonero¹, José Rodellar², Josep M. Rossell¹, Josep Rubió-Massegú¹



Abstract—This work presents an overview of some recent developments made by the authors in the field of vibrational control of large-scale structural systems subject to seismic excitations. The structural systems under consideration are classified in two broad categories: (i) high-rise buildings, and (ii) multi-building systems. When dealing with high-rise buildings, the inclusion principle can be used as a powerful mathematical tool to design semi-decentralized state-feedback and output-feedback controllers. In the case of multi-building systems, a passive-active structural vibration control for adjacent buildings consisting in a combination of passive linking elements with an active decentralized control system is designed. Numerical simulations show that the overall active-passive control system achieves excellent results when the active control system works; in case of full or partial failure of the active control system, a remarkable reduction in the vibrational response is guaranteed by the passive linking elements. Three different building models serve as example to clarify the theoretical results and, at the same time, to show the advantages of the proposed control approaches.

Index Terms—Building structures, structural vibration control, active-passive control, inclusion principle, decentralized control, output-feedback control, H-infinity control.

1 INTRODUCTION

The design and implementation of vibrational control systems for high-rise buildings and/or multi-building systems poses a variety of serious challenges, at both theoretical and practical level. Specifically, the latest trends in vibrational control of high-rise buildings involve multi-sensor systems, multi-actuator schemes based on magnetorheological semi-active dampers, and wireless communication networks [27]. Regarding to the multi-building case, the vibrational control has become a subject of increasing interest over the last years. This large-scale control problem may involve several buildings and typically presents a twofold goal: (i) minimizing the inter-story drifts to reduce building structural damages, and (ii) keeping the inter-building separations

to avoid inter-building collisions (pounding). Pounding may cause severe structural damage, even collapse in some extreme situations [1]. It is also worth to be noted that some seismic protection strategies such as passive base isolation, which can effectively reduce the seismic response of isolated buildings, may also increase the risk of pounding between insufficiently spaced adjacent structures [14].

In the high-rise building control problem, a first interesting approach consists in designing decentralized or semi-decentralized active control systems, where the actuation devices may be operated using local information provided by neighboring sensors and, consequently, helping to improve communication robustness and to achieve higher sampling frequencies in the real-time control operation. A second useful approach is the use of static output-feedback controllers, which only require a partial state knowledge. The basic contributions made by the authors in this context are related to the use of the *Inclusion Principle* in order to design semi-decentralized overlapping controllers [26], and may be summarized as follows: (i) study of several problems associated to the design of state-feedback overlapping controllers [16], [18], [19], [21], [22], (ii) extension of the *Inclusion Principle* to multi-overlapping problems [17], and (iii) design of semi-decentralized output-feedback H_∞ controllers [23].

In the multi-building control problem, the Connected Control Method (CCM) has recently been proposed as a viable means to protect connected flexible structures against earthquakes. The main idea in the CCM consists in linking together adjacent structures by means of coupling devices to provide appropriate reaction control forces which help to mitigate the vibrational response of the overall system. The application of the CCM using different kinds of passive, active, or semi-active control strategies have been investigated in [4], [5], [8], [9], [13], [15], [20], [25], [28], [29], [31]. In all these works, two-building systems are considered and the actuation devices are placed in the coupling elements. The works of the authors in this second field have been focused on the seismic response of a multi-building structure consisting of two adjacent actively controlled buildings linked by

¹Department of Applied Mathematics III, EPSEM-UPC, Campus Manresa, 08241-Manresa, Barcelona, Spain.

²Department of Applied Mathematics III, ETSECCPB-UPC, Campus Nord, C2, 08034-Barcelona, Spain.

E-mails: francisco.palacios@upc.edu, jose.rodellar@upc.edu, josep.maria.rossell@upc.edu, josep.rubio@upc.edu

damping passive elements. The resulting active-passive overall control system combines the high performance characteristics of active control systems with the reliability of passive control elements and, at the same time, admits a decentralized design and operation of the active control subsystems. The seismic response of the two-building system when the decentralized active control system is partially or totally switched off is a particularly relevant subject, which admits two interesting practical interpretations: from a reliability point of view, it can be seen as the system response under a partial or full failure of the active control system; from a design point of view, it can be understood as the response produced by different active control configurations corresponding to different levels of seismic protection.

To show the potential advantages of the proposed methodologies, three different building models have been considered: (1) a four-story building for the design of overlapping LQR controllers; (2) a five-story building, in the design of overlapping output-feedback H_∞ controllers; and (3) a two-building system, in the design of an active-passive control strategy for adjacent buildings. Numerical simulations of the vibrational response under a seismic excitation have been performed to assess the performance of the proposed control strategies.

2 BACKGROUND RESULTS

In this section, some basic definitions and results related to the Inclusion Principle and the design of overlapping controllers, in the case of two overlapping subsystems, are briefly presented. A rigorous treatment can be found in [2], [3], [7], [11], [12], [24], [26].

2.1 Inclusion Principle

Consider a pair of linear systems

$$\begin{aligned} \mathbf{S}: \dot{x}(t) &= A x(t) + B u(t), & \tilde{\mathbf{S}}: \dot{\tilde{x}}(t) &= \tilde{A} \tilde{x}(t) + \tilde{B} \tilde{u}(t), \\ y(t) &= C_y x(t), & \tilde{y}(t) &= \tilde{C}_y \tilde{x}(t), \end{aligned} \quad (1)$$

where $x(t) \in \mathbb{R}^n$, $u(t) \in \mathbb{R}^m$, $y(t) \in \mathbb{R}^l$ are the state, the input, and the output of \mathbf{S} at time $t \geq 0$ and $\tilde{x}(t) \in \mathbb{R}^{\tilde{n}}$, $\tilde{u}(t) \in \mathbb{R}^{\tilde{m}}$, $\tilde{y}(t) \in \mathbb{R}^{\tilde{l}}$ are the state, the input, and the output of $\tilde{\mathbf{S}}$. A , B , C_y and \tilde{A} , \tilde{B} , \tilde{C}_y are $n \times n$, $n \times m$, $l \times n$ and $\tilde{n} \times \tilde{n}$, $\tilde{l} \times \tilde{m}$ dimensional matrices, respectively. Suppose that the dimensions of the state, the input, and the output vectors $x(t)$, $u(t)$, $y(t)$ of \mathbf{S} are smaller than those of $\tilde{x}(t)$, $\tilde{u}(t)$, $\tilde{y}(t)$ of $\tilde{\mathbf{S}}$. Let $x(t; x_0, u)$ and $y[x(t)]$ denote the state behavior and the corresponding output of \mathbf{S} for a fixed input $u(t)$ and for an initial state $x(0) = x_0$, respectively. Similar notations $\tilde{x}(t; \tilde{x}_0, \tilde{u})$ and $\tilde{y}[\tilde{x}(t)]$ are used for the state behavior and output of system $\tilde{\mathbf{S}}$.

Let us consider the following linear transformations:

$$\begin{aligned} V: \mathbb{R}^n &\longrightarrow \mathbb{R}^{\tilde{n}}, & U: \mathbb{R}^{\tilde{m}} &\longrightarrow \mathbb{R}^m, \\ R: \mathbb{R}^m &\longrightarrow \mathbb{R}^{\tilde{m}}, & Q: \mathbb{R}^{\tilde{m}} &\longrightarrow \mathbb{R}^m, \\ T: \mathbb{R}^l &\longrightarrow \mathbb{R}^{\tilde{l}}, & S: \mathbb{R}^{\tilde{l}} &\longrightarrow \mathbb{R}^l, \end{aligned} \quad (2)$$

where $\text{rank}(V) = n$, $\text{rank}(R) = m$, $\text{rank}(T) = l$ and such that $UV = I_n$, $QR = I_m$, $ST = I_l$, where I_n , I_m , I_l are the identity matrices of indicated dimensions.

Definition 1: (Inclusion Principle) A system $\tilde{\mathbf{S}}$ includes the system \mathbf{S} if there exists a quadruplet of matrices (U, V, R, S) such that, for any initial state x_0 and any fixed input $u(t)$ of \mathbf{S} , the choice

$$\begin{aligned} \tilde{x}_0 &= V x_0, \\ \tilde{u}(t) &= R u(t), \quad \text{for all } t \geq 0 \end{aligned}$$

of the initial state \tilde{x}_0 and input $\tilde{u}(t)$ of the system $\tilde{\mathbf{S}}$, implies

$$\begin{aligned} x(t; x_0, u) &= U \tilde{x}(t; \tilde{x}_0, \tilde{u}), \\ y[x(t)] &= S \tilde{y}[\tilde{x}(t)], \quad \text{for all } t \geq 0. \end{aligned}$$

Suppose that the pairs of matrices (U, V) , (Q, R) and (S, T) are given. Then, the expanded matrices \tilde{A} , \tilde{B} , and \tilde{C}_y can be expressed as

$$\tilde{A} = V A U + M, \quad \tilde{B} = V B Q + N, \quad \tilde{C}_y = T C_y U + L, \quad (3)$$

where M , N and L are complementary matrices of appropriate dimensions. In terms of complementary matrices, the inclusion principle can be established in the following way.

Theorem 1: A system $\tilde{\mathbf{S}}$ includes the system \mathbf{S} if and only if $U M^i V = 0$, $U M^{i-1} N R = 0$, $S L M^{i-1} V = 0$ and $S L M^{i-1} N R = 0$ for all $i = 1, 2, \dots, \tilde{n}$.

There are two principal forms of the inclusion principle, which are called *restrictions* and *aggregations* [26]. In this paper, only restrictions will be used.

Proposition 1: A system \mathbf{S} is a restriction of the system $\tilde{\mathbf{S}}$ if and only if $M V = 0$, $N R = 0$ and $L V = 0$.

Let us suppose that the system \mathbf{S} given in (1) admits an overlapping decomposition. In terms of the system matrices, this assumption means that A , B and C_y present a block tridiagonal structure

$$\begin{aligned} A &= \begin{bmatrix} A_{11} & A_{12} & 0 \\ A_{21} & A_{22} & A_{23} \\ 0 & A_{32} & A_{33} \end{bmatrix}, & B &= \begin{bmatrix} B_{11} & B_{12} & 0 \\ B_{21} & B_{22} & B_{23} \\ 0 & B_{32} & B_{33} \end{bmatrix}, \\ C_y &= \begin{bmatrix} (C_y)_{11} & (C_y)_{12} & 0 \\ (C_y)_{21} & (C_y)_{22} & (C_y)_{23} \\ 0 & (C_y)_{32} & (C_y)_{33} \end{bmatrix}, \end{aligned}$$

where A_{ij} , B_{ij} , $(C_y)_{ij}$, for $i, j = 1, 2, 3$, are $n_i \times n_i$, $n_i \times m_j$, $l_i \times n_j$ dimensional matrices, respectively. The partition of the state $x = (x_1^T, x_2^T, x_3^T)^T$ has components of respective dimensions n_1, n_2, n_3 , satisfying $n_1 + n_2 + n_3 = n$; the partition of $u = (u_1^T, u_2^T, u_3^T)^T$ has components of dimensions m_1, m_2, m_3 , such that $m_1 + m_2 + m_3 = m$; and $y = (y_1^T, y_2^T, y_3^T)^T$ has components of respective dimensions l_1, l_2, l_3 , satisfying $l_1 + l_2 + l_3 = l$.

The controller design starts with the definition of the expansion transformations

$$V = \begin{bmatrix} I_{n_1} & 0 & 0 \\ 0 & I_{n_2} & 0 \\ 0 & 0 & I_{n_3} \end{bmatrix}, \quad R = \begin{bmatrix} I_{m_1} & 0 & 0 \\ 0 & I_{m_2} & 0 \\ 0 & 0 & I_{m_3} \end{bmatrix}, \quad T = \begin{bmatrix} I_{l_1} & 0 & 0 \\ 0 & I_{l_2} & 0 \\ 0 & 0 & I_{l_3} \end{bmatrix}$$

and their corresponding pseudoinverse contractions

$$U = \begin{bmatrix} I_{n_1} & 0 & 0 & 0 \\ 0 & \frac{1}{2}I_{n_2} & \frac{1}{2}I_{n_2} & 0 \\ 0 & 0 & 0 & I_{n_3} \end{bmatrix}, \quad Q = \begin{bmatrix} I_{m_1} & 0 & 0 & 0 \\ 0 & \frac{1}{2}I_{m_2} & \frac{1}{2}I_{m_2} & 0 \\ 0 & 0 & 0 & I_{m_3} \end{bmatrix},$$

$$S = \begin{bmatrix} I_{l_1} & 0 & 0 & 0 \\ 0 & \frac{1}{2}I_{l_2} & \frac{1}{2}I_{l_2} & 0 \\ 0 & 0 & 0 & I_{l_3} \end{bmatrix},$$

where $U=(V^T V)^{-1}V^T$, $Q=(R^T R)^{-1}R^T$, $S=(T^T T)^{-1}T^T$. Then, the expanded matrices $\bar{A}=VAU$, $\bar{B}=VBQ$, $\bar{C}_y=TC_yU$, have the form

$$\bar{A} = \begin{bmatrix} A_{11} & \frac{1}{2}A_{12} & \frac{1}{2}A_{12} & 0 \\ A_{21} & \frac{1}{2}A_{22} & \frac{1}{2}A_{22} & A_{23} \\ A_{21} & \frac{1}{2}A_{22} & \frac{1}{2}A_{22} & A_{23} \\ 0 & \frac{1}{2}A_{32} & \frac{1}{2}A_{32} & A_{33} \end{bmatrix},$$

$$\bar{B} = \begin{bmatrix} B_{11} & \frac{1}{2}B_{12} & \frac{1}{2}B_{12} & 0 \\ B_{21} & \frac{1}{2}B_{22} & \frac{1}{2}B_{22} & B_{23} \\ B_{21} & \frac{1}{2}B_{22} & \frac{1}{2}B_{22} & B_{23} \\ 0 & \frac{1}{2}B_{32} & \frac{1}{2}B_{32} & B_{33} \end{bmatrix},$$

$$\bar{C}_y = \begin{bmatrix} (C_y)_{11} & \frac{1}{2}(C_y)_{12} & \frac{1}{2}(C_y)_{12} & 0 \\ (C_y)_{21} & \frac{1}{2}(C_y)_{22} & \frac{1}{2}(C_y)_{22} & (C_y)_{23} \\ (C_y)_{21} & \frac{1}{2}(C_y)_{22} & \frac{1}{2}(C_y)_{22} & (C_y)_{23} \\ 0 & \frac{1}{2}(C_y)_{32} & \frac{1}{2}(C_y)_{32} & (C_y)_{33} \end{bmatrix}.$$

In order to get an almost-decoupled expanded system, we add complementary matrices as indicated in (3). These complementary matrices can be chosen in the form

$$M = \begin{bmatrix} 0 & \frac{1}{2}A_{12} & -\frac{1}{2}A_{12} & 0 \\ 0 & \frac{1}{2}A_{22} & -\frac{1}{2}A_{22} & 0 \\ 0 & -\frac{1}{2}A_{22} & \frac{1}{2}A_{22} & 0 \\ 0 & -\frac{1}{2}A_{32} & \frac{1}{2}A_{32} & 0 \end{bmatrix}, \quad N = \begin{bmatrix} 0 & \frac{1}{2}B_{12} & -\frac{1}{2}B_{12} & 0 \\ 0 & \frac{1}{2}B_{22} & -\frac{1}{2}B_{22} & 0 \\ 0 & -\frac{1}{2}B_{22} & \frac{1}{2}B_{22} & 0 \\ 0 & -\frac{1}{2}B_{32} & \frac{1}{2}B_{32} & 0 \end{bmatrix},$$

$$L = \begin{bmatrix} 0 & \frac{1}{2}(C_y)_{12} & -\frac{1}{2}(C_y)_{12} & 0 \\ 0 & \frac{1}{2}(C_y)_{22} & -\frac{1}{2}(C_y)_{22} & 0 \\ 0 & -\frac{1}{2}(C_y)_{22} & \frac{1}{2}(C_y)_{22} & 0 \\ 0 & -\frac{1}{2}(C_y)_{32} & \frac{1}{2}(C_y)_{32} & 0 \end{bmatrix},$$

resulting

$$\tilde{A} = \bar{A} + M = \begin{bmatrix} \tilde{A}_{11} & \tilde{A}_{12} \\ \tilde{A}_{21} & \tilde{A}_{22} \end{bmatrix} = \begin{bmatrix} A_{11} & A_{12} & 0 & 0 \\ A_{21} & A_{22} & 0 & A_{23} \\ A_{21} & 0 & A_{22} & A_{23} \\ 0 & 0 & A_{32} & A_{33} \end{bmatrix},$$

$$\tilde{B} = \bar{B} + N = \begin{bmatrix} \tilde{B}_{11} & \tilde{B}_{12} \\ \tilde{B}_{21} & \tilde{B}_{22} \end{bmatrix} = \begin{bmatrix} B_{11} & B_{12} & 0 & 0 \\ B_{21} & B_{22} & 0 & B_{23} \\ B_{21} & 0 & B_{22} & B_{23} \\ 0 & 0 & B_{32} & B_{33} \end{bmatrix},$$

$$\tilde{C}_y = \bar{C}_y + L = \begin{bmatrix} (\tilde{C}_y)_{11} & (\tilde{C}_y)_{12} \\ (\tilde{C}_y)_{21} & (\tilde{C}_y)_{22} \end{bmatrix} = \begin{bmatrix} (C_y)_{11} & (C_y)_{12} & 0 & 0 \\ (C_y)_{21} & (C_y)_{22} & 0 & (C_y)_{23} \\ (C_y)_{21} & 0 & (C_y)_{22} & (C_y)_{23} \\ 0 & 0 & (C_y)_{32} & (C_y)_{33} \end{bmatrix}.$$

The expanded system can be denoted by

$$\tilde{\mathbf{S}} : \dot{\tilde{x}}(t) = \tilde{A} \tilde{x}(t) + \tilde{B} \tilde{u}(t),$$

$$\tilde{y}(t) = \tilde{C}_y \tilde{x}(t),$$

with $\tilde{x}^T = (x_1^T, x_2^T, x_2^T, x_3^T)$, $\tilde{u}^T = (u_1^T, u_2^T, u_2^T, u_3^T)$ and $\tilde{y}^T = (y_1^T, y_2^T, y_2^T, y_3^T)$. Using the block notation given in (4), we can write

$$\tilde{\mathbf{S}}_1 : \dot{\tilde{x}}_1(t) = \tilde{A}_{11} \tilde{x}_1(t) + \tilde{B}_{11} \tilde{u}_1(t) + \tilde{A}_{12} \tilde{x}_2(t) + \tilde{B}_{12} \tilde{u}_2(t),$$

$$\tilde{y}_1(t) = (\tilde{C}_y)_{11} \tilde{x}_1(t) + (\tilde{C}_y)_{12} \tilde{x}_2(t),$$

$$\tilde{\mathbf{S}}_2 : \dot{\tilde{x}}_2(t) = \tilde{A}_{22} \tilde{x}_2(t) + \tilde{B}_{22} \tilde{u}_2(t) + \tilde{A}_{21} \tilde{x}_1(t) + \tilde{B}_{21} \tilde{u}_1(t),$$

$$\tilde{y}_2(t) = (\tilde{C}_y)_{21} \tilde{x}_1(t) + (\tilde{C}_y)_{22} \tilde{x}_2(t),$$

where $\tilde{x}_1^T = (x_1^T, x_2^T)$, $\tilde{u}_1^T = (u_1^T, u_2^T)$, $\tilde{y}_1^T = (y_1^T, y_2^T)$, $\tilde{x}_2^T = (x_2^T, x_3^T)$, $\tilde{u}_2^T = (u_2^T, u_3^T)$, $\tilde{y}_2^T = (y_2^T, y_3^T)$. By removing the interconnection blocks, two decoupled expanded subsystems result

$$\tilde{\mathbf{S}}_D^{(1)} : \dot{\tilde{x}}_1(t) = \tilde{A}_{11} \tilde{x}_1(t) + \tilde{B}_{11} \tilde{u}_1(t),$$

$$\tilde{y}_1(t) = (\tilde{C}_y)_{11} \tilde{x}_1(t),$$

$$\tilde{\mathbf{S}}_D^{(2)} : \dot{\tilde{x}}_2(t) = \tilde{A}_{22} \tilde{x}_2(t) + \tilde{B}_{22} \tilde{u}_2(t),$$

$$\tilde{y}_2(t) = (\tilde{C}_y)_{22} \tilde{x}_2(t),$$

which define a decoupled expanded system

$$\tilde{\mathbf{S}}_D : \dot{\tilde{x}}(t) = \tilde{A}_D \tilde{x}(t) + \tilde{B}_D \tilde{u}(t),$$

$$\tilde{y}(t) = (\tilde{C}_y)_D \tilde{x}(t),$$

where $\tilde{A}_D = \text{diag}\{\tilde{A}_{11}, \tilde{A}_{22}\}$, $\tilde{B}_D = \text{diag}\{\tilde{B}_{11}, \tilde{B}_{22}\}$ and $(\tilde{C}_y)_D = \text{diag}\{(\tilde{C}_y)_{11}, (\tilde{C}_y)_{22}\}$. At this point, we have to design a decentralized controller $\tilde{u}_D(t)$ for $\tilde{\mathbf{S}}_D$. This can be done by independently computing local controllers for $\tilde{\mathbf{S}}_D^{(1)}$ and $\tilde{\mathbf{S}}_D^{(2)}$ given in (5). In this paper, two kinds of controllers will be considered: (i) state-feedback controllers, and (ii) output-feedback controllers. For each one of them, the contractibility conditions have to be stated.

Definition 2: (State Contractibility) Suppose that $\tilde{\mathbf{S}}$ is an expansion of the system \mathbf{S} . Then, a control law $\tilde{u}(t) = \tilde{K} \tilde{x}(t)$ for $\tilde{\mathbf{S}}$ is contractible to the control law $u(t) = Kx(t)$ for \mathbf{S} if there exist transformations as in (2) such that, for any initial state $x_0 \in \mathbb{R}^n$ and any input $u(t) \in \mathbb{R}^m$, the choice

$$\tilde{x}_0 = Vx_0,$$

$$\tilde{u}(t) = Ru(t), \quad \text{for all } t \geq 0$$

of the initial state \tilde{x}_0 and input $\tilde{u}(t)$ of the system $\tilde{\mathbf{S}}$, implies

$$Kx(t; x_0, u) = Q\tilde{K}\tilde{x}(t; Vx_0, Ru), \quad \text{for all } t \geq 0.$$

Proposition 2: Suppose that \mathbf{S} is a restriction of the system $\tilde{\mathbf{S}}$. Then, a control law $\tilde{u}(t) = \tilde{K} \tilde{x}(t)$ for $\tilde{\mathbf{S}}$ is contractible to the control law $u(t) = Kx(t)$ for \mathbf{S} if $K = Q\tilde{K}V$.

Definition 3: (Output Contractibility) Suppose that $\tilde{\mathbf{S}}$ is an expansion of the system \mathbf{S} . Then, a control law $\tilde{u}(t) = \tilde{K} \tilde{y}(t)$ for $\tilde{\mathbf{S}}$ is contractible to the control law $u(t) = Ky(t)$ for \mathbf{S} if there exist transformations as in (2)

(4)

such that, for any initial state $x_0 \in \mathbb{R}^n$ and any input $u(t) \in \mathbb{R}^m$ the choice

$$\begin{aligned}\tilde{x}_0 &= Vx_0, \\ \tilde{u}(t) &= Ru(t), \text{ for all } t \geq 0\end{aligned}$$

of the initial state \tilde{x}_0 and input $\tilde{u}(t)$ of the system $\tilde{\mathbf{S}}$, implies

$$Ky[x(t; x_0, u)] = Q\tilde{K}\tilde{y}[\tilde{x}(t; Vx_0, Ru)], \text{ for all } t \geq 0.$$

Proposition 3: Suppose that \mathbf{S} is a restriction of the system $\tilde{\mathbf{S}}$. Then, a control law $\tilde{u}(t) = \tilde{K}\tilde{y}(t)$ for $\tilde{\mathbf{S}}$ is contractible to the control law $u(t) = Ky(t)$ for \mathbf{S} if $K = Q\tilde{K}T$.

According to Definition 2, a state-feedback controller $\tilde{u}_D(t) = \tilde{K}_D \tilde{x}(t)$ is contracted to an overlapping controller $u(t) = K_o x(t)$ to be implemented into the original system \mathbf{S} . Analogously, by Definition 3, an output-feedback controller $\tilde{u}_D(t) = \tilde{K}_D \tilde{y}(t)$ is contracted to an overlapping controller $u(t) = K_o y(t)$. In both cases, the corresponding contracted gain matrices have the following block diagonal form:

$$K_o = \begin{bmatrix} K_{11} & K_{12} & 0 \\ K_{21} & K_{22} & K_{23} \\ 0 & K_{32} & K_{33} \end{bmatrix}.$$

We can note that the design of overlapping controllers, using the inclusion principle, has two main features: (i) *structure*, which means that the resulting controller fits in with the system structure, and (ii) *lower dimensionality*, that is, the gain matrix K_o is computed from two lower-dimension controllers which are independently designed.

2.2 Controller design for two overlapping subsystems

In this subsection an overlapping state-feedback LQR controller will be designed. To this end, we start by designing two independent local state-feedback LQR controllers for the expanded decoupled subsystems $\tilde{\mathbf{S}}_D^{(1)}$ and $\tilde{\mathbf{S}}_D^{(2)}$. Let us consider the local quadratic cost functions

$$\begin{aligned}\tilde{J}_D^{(1)}(\tilde{x}_{10}, \tilde{u}_1(t)) &= \int_0^\infty \left[\tilde{x}_1^T(t) \tilde{Q}_1^* \tilde{x}_1(t) + \tilde{u}_1^T(t) \tilde{R}_1^* \tilde{u}_1(t) \right] dt, \\ \tilde{J}_D^{(2)}(\tilde{x}_{20}, \tilde{u}_2(t)) &= \int_0^\infty \left[\tilde{x}_2^T(t) \tilde{Q}_2^* \tilde{x}_2(t) + \tilde{u}_2^T(t) \tilde{R}_2^* \tilde{u}_2(t) \right] dt,\end{aligned}\quad (6)$$

where \tilde{x}_{10} and \tilde{x}_{20} are the initial states of $\tilde{\mathbf{S}}_D^{(1)}$ and $\tilde{\mathbf{S}}_D^{(2)}$, respectively, and \tilde{Q}_1^* , \tilde{Q}_2^* , \tilde{R}_1^* and \tilde{R}_2^* are appropriate expanded matrices. The gain matrices for the control laws that minimize the cost functions (6)

$$\tilde{u}_1(t) = \tilde{K}_1 \tilde{x}_1(t), \quad \tilde{u}_2(t) = \tilde{K}_2 \tilde{x}_2(t),$$

can be independently computed as

$$\tilde{K}_1 = \left[\tilde{R}_1^* \right]^{-1} \tilde{B}_1^T \tilde{P}_1, \quad \tilde{K}_2 = \left[\tilde{R}_2^* \right]^{-1} \tilde{B}_2^T \tilde{P}_2,$$

where \tilde{P}_1 and \tilde{P}_2 are the solutions of the corresponding Riccati equations. In the decoupled expanded system $\tilde{\mathbf{S}}_D$,

the gain matrix of the controller $\tilde{u}(t) = \tilde{K}_D \tilde{x}(t)$ minimizing the cost function

$$\tilde{J}_D(\tilde{x}_0, \tilde{u}(t)) = \int_0^\infty \left[\tilde{x}^T(t) \tilde{Q}_D^* \tilde{x}(t) + \tilde{u}^T(t) \tilde{R}_D^* \tilde{u}(t) \right] dt,$$

with $\tilde{Q}_D^* = \text{diag}\{\tilde{Q}_1^*, \tilde{Q}_2^*\}$, $\tilde{R}_D^* = \text{diag}\{\tilde{R}_1^*, \tilde{R}_2^*\}$, can be written as a block diagonal gain matrix $\tilde{K}_D^* = \text{diag}\{\tilde{K}_1^*, \tilde{K}_2^*\}$. Finally, the controller $\tilde{u}_D(t) = \tilde{K}_D \tilde{x}(t)$ is contracted to an overlapping controller $u(t) = K_o x(t)$ to be implemented into the original system \mathbf{S} .

2.3 Sequential decomposition

When dealing with large-scale systems, they are usually composed by a large number of subsystems. In this subsection, we will use the inclusion principle to carry out a multi-step expansion that allows the decentralized design of a sequence of expanded local controllers. The obtained local controllers are subsequently contracted to produce a multi-overlapping controller which can be implemented in the original system.

Having this idea in mind, let us consider a system

$$\mathbf{S} : \dot{x}(t) = Ax(t) + Bu(t)$$

formed by $(r+1)$ overlapping subsystems

$$\mathbf{S}^{(j)} : \dot{x}^{(j)}(t) = A^{(j)}x^{(j)}(t) + B^{(j)}u^{(j)}(t), \quad j = 1, \dots, r+1.$$

The system matrix A has the block structure shown in Fig. 1 with $(r+1)$ main blocks $A^{(j)}$ and r overlapping sub-blocks $O_A^{(j)}$. The input matrix B presents an analogous structure.

Broadly speaking, the basic idea is to consider the first r subsystems as a single subsystem which overlaps with $\mathbf{S}^{(r+1)}$. Then, the standard theory for two overlapped systems may be applied to obtain an expanded space, where a local controller can be designed for the expanded subsystem $\tilde{\mathbf{S}}^{(r+1)}$. This step also produces another expanded system with only r overlapped subsystems. After r expansion steps, two non-overlapped expanded subsystems result and the design of $(r+1)$ expanded local controllers can be completed. Finally, a sequence of r contraction steps on the expanded local controllers yields an overlapping global controller for the initial system. For the subsystem $\mathbf{S}^{(j)}$, the state and the input dimensions are respectively denoted by $d_x^{(j)}$ and $d_u^{(j)}$; $A^{(j)}$ is a square matrix of dimension $d_x^{(j)}$, and $B^{(j)}$ is a $d_x^{(j)} \times d_u^{(j)}$ matrix. As for the overlapping blocks, $O_A^{(j)}$ is a square matrix of dimension $o_x^{(j)}$, and $O_B^{(j)}$ is a $o_x^{(j)} \times o_u^{(j)}$ matrix. Note that some of the numbers $o_u^{(j)}$ may be zero. This is the case when there is no control overlapping between subsystems $\mathbf{S}^{(j)}$ and $\mathbf{S}^{(j+1)}$. For $j=1, \dots, r$, we also define the numbers

$$\begin{cases} n_1^{(j)} = \sum_{i=1}^j (d_x^{(i)} - o_x^{(i)}) \\ n_2^{(j)} = o_x^{(j)} \\ n_3^{(j)} = d_x^{(j+1)} - o_x^{(j)} \end{cases} \begin{cases} m_1^{(j)} = \sum_{i=1}^j (d_u^{(i)} - o_u^{(i)}) \\ m_2^{(j)} = o_u^{(j)} \\ m_3^{(j)} = d_u^{(j+1)} - o_u^{(j)} \end{cases}$$

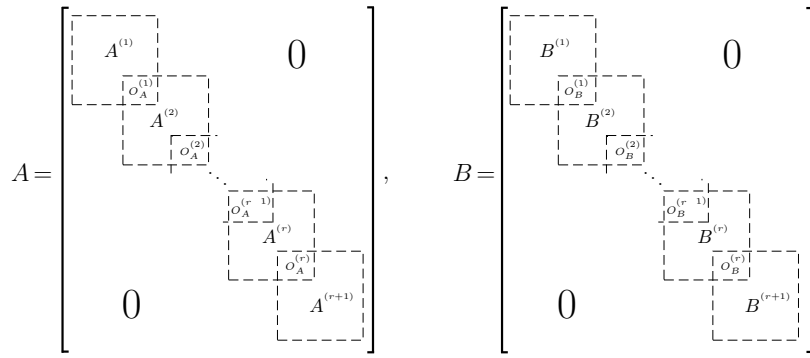


Fig. 1. Block structures of matrices A and B .

We start with the pair $P_1^{(r+1)}=(A, B)$ and consider the expansion matrices

$$V^{(r)} = \begin{bmatrix} I_{n_1^{(r)}} & 0 & 0 \\ 0 & I_{n_2^{(r)}} & 0 \\ 0 & 0 & I_{n_3^{(r)}} \end{bmatrix}, \quad R^{(r)} = \begin{bmatrix} I_{m_1^{(r)}} & 0 & 0 \\ 0 & I_{m_2^{(r)}} & 0 \\ 0 & 0 & I_{m_3^{(r)}} \end{bmatrix},$$

to perform an overlapping decomposition of $P_1^{(r+1)}$ as described in Subsection 2.1, obtaining the decoupled pairs

$$P_1^{(r)} = (\tilde{A}_1^{(r)}, \tilde{B}_1^{(r)}), \quad P_2^{(r+1)} = (\tilde{A}_1^{(r+1)}, \tilde{B}_1^{(r+1)}),$$

as illustrated in Fig. 2. The pair $P_2^{(r+1)}$ contains no over-

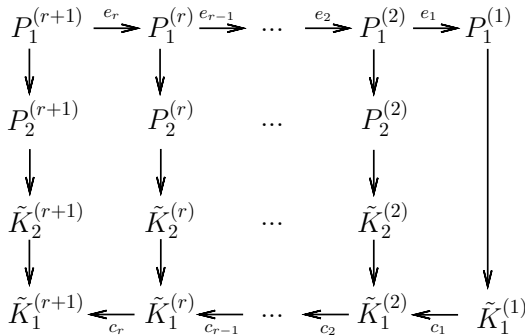


Fig. 2. Sequential overlapping decomposition scheme.

lapping blocks and a gain matrix $\tilde{K}_2^{(r+1)}$ can be directly designed. The other pair $P_1^{(r)}$ contains r subsystems with $(r - 1)$ overlapping blocks and the process needs to be repeated until a fully decoupled expansion results. More precisely, the expansion process involves $(r + 1)$ pairs $P_1^{(j)}$ and it is carried out in r steps by decreasing the index j from $(r + 1)$ to 1. The expansion step j starts with the pair $P_1^{(j+1)}$, that describes a system with $(j + 1)$ subsystems and j overlapping blocks, and it uses expansion matrices $V^{(j)}$ and $R^{(j)}$ to yield the expanded pairs

$$P_1^{(j)} = (\tilde{A}_1^{(j)}, \tilde{B}_1^{(j)}), \quad P_2^{(j+1)} = (\tilde{A}_1^{(j+1)}, \tilde{B}_1^{(j+1)}).$$

A gain matrix $\tilde{K}_2^{(j+1)}$ is computed for the expanded system with no overlapping blocks $P_2^{(j+1)}$ while the pair $P_1^{(j)}$, which contains j subsystems and $(j - 1)$ overlapping blocks, is supplied as the starting point to the next expansion step. After r expansion steps, an expanded non-overlapped pair $P_1^{(1)}$ results, and a gain matrix $\tilde{K}_1^{(1)}$ is directly computed. The matrix $\bar{K}^{(1)}=\text{diag}(\tilde{K}_1^{(1)}, \tilde{K}_2^{(2)})$ can be contracted to obtain an overlapping controller $\tilde{K}_1^{(2)}= Q^{(1)}\bar{K}^{(1)}V^{(1)}$ for the expanded pair $P_1^{(2)}$. The contraction step j starts with the expanded gain matrix $\tilde{K}_1^{(j)}$ and it uses $\tilde{K}_2^{(j+1)}$ to build $\bar{K}^{(j)}=\text{diag}(\tilde{K}_1^{(j)}, \tilde{K}_2^{(j+1)})$ and to compute the overlapping controller $\tilde{K}_1^{(j+1)}= Q^{(j)}\bar{K}^{(j)}V^{(j)}$. After r contraction steps, an overlapping gain matrix $K=\tilde{K}_1^{(r+1)}$ for the original system results.

The diagram in Fig. 2 shows schematically the whole procedure. The process starts with $P_1^{(r+1)}$ and the expansion progresses along the top from left to right. Note that a gain matrix $\tilde{K}_2^{(j+1)}$ is computed at each step. However, the expansion process needs to be completed before the first gain matrix $\tilde{K}_1^{(1)}$ is computed. Then, the contraction process progresses from right to left along the bottom, generating in each step the gain matrix $\tilde{K}_1^{(j+1)}$.

3 EXAMPLE: FOUR-STORY BUILDING MODEL

To show the potential advantages of the proposed control approach and to illustrate more clearly the details of the sequential design procedure presented in the previous section, we consider the problem of reducing the vibrational response of a tall building under an earthquake excitation. More precisely, a simplified one-dimensional model of a four-story building has been selected. The control goal is to reduce the inter-story drifts when the building is subjected to a ground seismic excitation. To this end, two different actuation schemes have been considered: (a) inter-story cross-actuators, and (b) direct actuators (see Fig. 3). First, the building is considered as a whole and, for each actuation scheme, a centralized optimal LQR state feedback controller is designed. These centralized controllers will later be taken as a reference to evaluate the performance of the

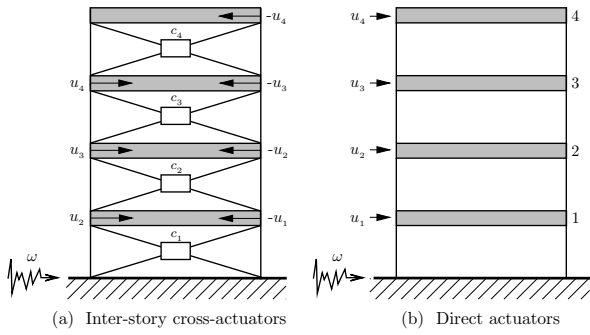


Fig. 3. Two actuation schemes for a four-story building.

overlapping controllers. Secondly, the building is seen as made up of three overlapped subsystems, which include two consecutive stories, that is: $\mathbf{S}^{(1)}=[1, 2]$, $\mathbf{S}^{(2)}=[2, 3]$, $\mathbf{S}^{(3)}=[3, 4]$ (see Fig. 4). A sequential overlapping decom-

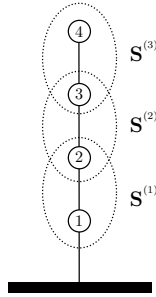


Fig. 4. Multi-overlapping decomposition for a four-story building.

position is then applied to this multi-overlapped system in order to obtain a multi-overlapping controller for each actuation scheme.

3.1 State space model

The motion of the four-story building can be described by the second-order differential equation

$$\mathbf{M}\ddot{q}(t) + \mathbf{C}\dot{q}(t) + \mathbf{K}q(t) = \mathbf{T}_u u(t) + \mathbf{T}_w w(t), \quad (7)$$

where $q(t) \in \mathbb{R}^4$ is the displacement vector relative to the ground, \mathbf{M} , \mathbf{C} , \mathbf{K} , are the mass, damping, and stiffness matrices, respectively, (see Fig. 5). The vector $u(t) \in \mathbb{R}^4$ is the control force, $w(t) \in \mathbb{R}$ is the ground acceleration, \mathbf{T}_u is the control location matrix, and \mathbf{T}_w is the excitation location matrix.

The particular values of the matrices that will be used to calculate the controllers and to carry out the simulations are the following:

$$\begin{aligned} \mathbf{M} &= 10^2 \times \text{diag} [3456, 3456, 3456, 3456], \\ \mathbf{C} &= 10^3 \times \begin{bmatrix} 5874 & -2937 & 0 & 0 \\ -2937 & 5874 & -2937 & 0 \\ 0 & -2937 & 5874 & -2937 \\ 0 & 0 & -2937 & 2937 \end{bmatrix}, \\ \mathbf{K} &= 10^5 \times \begin{bmatrix} 6808 & -3404 & 0 & 0 \\ -3404 & 6808 & -3404 & 0 \\ 0 & -3404 & 6808 & -3404 \\ 0 & 0 & -3404 & 3404 \end{bmatrix}, \\ \mathbf{T}_w &= -\mathbf{M}[1, 1, 1, 1]^T, \end{aligned} \quad (8)$$

where masses are in kg , damping coefficients are in $N \cdot s/m$, and stiffness coefficients are in N/m . As for the control location, two different matrices are considered

$$\mathbf{T}_u^{(a)} = \begin{bmatrix} -1 & 1 & 0 & 0 \\ 0 & -1 & 1 & 0 \\ 0 & 0 & -1 & 1 \\ 0 & 0 & 0 & -1 \end{bmatrix}, \quad \mathbf{T}_u^{(b)} = \begin{bmatrix} 1 & 0 & 0 & 0 \\ 0 & 1 & 0 & 0 \\ 0 & 0 & 1 & 0 \\ 0 & 0 & 0 & 1 \end{bmatrix},$$

corresponding, respectively, to the actuation schemes (a) and (b) shown in Fig. 3.

From the second-order model (7), a first-order state-space model can be derived

$$\mathbf{S}: \dot{x}(t) = \mathbf{A}x(t) + \mathbf{B}^{(j)}u(t) + \mathbf{E}w(t),$$

where the state vector $x(t) \in \mathbb{R}^8$ contains the inter-story drifts and velocities arranged in increasing order (see Fig. 5), that is,

$$x(t) = [q_1, \dot{q}_1, (q_2 - q_1), (\dot{q}_2 - \dot{q}_1), \dots, (q_4 - q_3), (\dot{q}_4 - \dot{q}_3)]^T.$$

A detailed derivation of the first-order state-space model

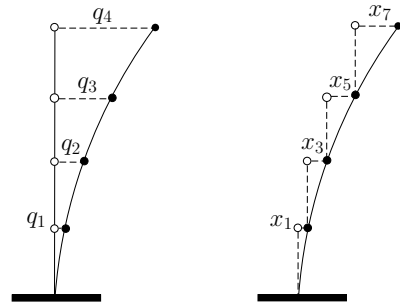


Fig. 5. Absolute and relative displacements.

can be found in [27]. For the particular values corresponding to (8), the state matrix is

$$\mathbf{A} = 10^3 \times \begin{bmatrix} 0 & 0.0010 & 0 & 0 & 0 & 0 & 0 & 0 \\ -0.9850 & -0.0085 & 0.9850 & 0.0085 & 0 & 0 & 0 & 0 \\ 0 & 0 & 0 & 0.0010 & 0 & 0 & 0 & 0 \\ 0.9850 & 0.0085 & -1.9699 & -0.0170 & 0.9850 & 0.0085 & 0 & 0 \\ 0 & 0 & 0 & 0 & 0 & 0.0010 & 0 & 0 \\ 0 & 0 & 0.9850 & 0.0085 & -1.9699 & -0.0170 & 0.9850 & 0.0085 \\ 0 & 0 & 0 & 0 & 0 & 0 & 0 & 0.0010 \\ 0 & 0 & 0 & 0 & 0.9850 & 0.0085 & -1.9699 & -0.0170 \end{bmatrix},$$

the input matrix is given by

$$\mathbf{E} = [0, -1, 0, 0, 0, 0, 0, 0]^T,$$

the control matrix for the inter-story actuation scheme is

$$\mathbf{B}^{(a)} = 10^{-5} \times \begin{bmatrix} 0 & 0 & 0 & 0 \\ -0.2894 & 0.2894 & 0 & 0 \\ 0 & 0 & 0 & 0 \\ 0.2894 & -0.5787 & 0.2894 & 0 \\ 0 & 0 & 0 & 0 \\ 0 & 0.2894 & -0.5787 & 0.2894 \\ 0 & 0 & 0 & 0 \\ 0 & 0 & 0.2894 & -0.5787 \end{bmatrix},$$

while the control matrix for the direct actuation scheme is

$$\mathbf{B}^{(b)} = 10^{-5} \times \begin{bmatrix} 0 & 0 & 0 & 0 \\ 0.2894 & 0 & 0 & 0 \\ 0 & 0 & 0 & 0 \\ -0.2894 & 0.2894 & 0 & 0 \\ 0 & 0 & 0 & 0 \\ 0 & -0.2894 & 0.2894 & 0 \\ 0 & 0 & 0 & 0 \\ 0 & 0 & -0.2894 & 0.2894 \end{bmatrix}.$$

3.2 Centralized controllers

To compute a centralized optimal LQR state feedback controller, we consider the quadratic index

$$J_c(x(t), u(t)) = \int_0^\infty [x^T(t)Q^*x(t) + u^T(t)R^*u(t)] dt, \quad (9)$$

defined by the weighting matrices $Q^*=I_8$, $R^*=10^{-15} I_4$. Using the Matlab command `lqr()` with system matrices A and $B^{(a)}$, we obtain a centralized gain matrix $K_c^{(a)}$ given in Fig. 16 for the case of inter-story cross-actuators. The optimal cost $[J_c^{(a)}]_{opt} = 39.58$ is computed as the trace of the matrix $P^{(a)}$, which is obtained as the solution of the corresponding Riccati equation.

In the case of direct actuators, the system matrices A and $B^{(b)}$ are used to yield a centralized gain matrix $K_c^{(b)}$, also given in Fig. 16, with an optimal cost $[J_c^{(b)}]_{opt} = 45.06$.

Remark 1: It is worth noting that the gain matrix $K_c^{(a)}$, obtained in the case of inter-story actuators, exhibits an almost-decentralized structure. This fact can be explained by the particular structure of the physical system and the actuation scheme. In this case, a multi-overlapping controller, or even a decentralized controller, could be obtained by removing some almost-zero elements. The structured controller so obtained is a small perturbation of the optimal controller, and it is reasonable to expect that it will present a good performance. However, it must be emphasized that even in this extremely favorable case, a centralized controller needs to be previously computed in order to apply this strategy. Of course, this approach cannot be applied to the case of direct actuators, where a full gain matrix $K_c^{(b)}$ has been obtained.

3.3 Multi-overlapping controllers

Inter-story actuators. Let us consider the main system $S^{(a)}$ defined by the pair $(A, B^{(a)})$. We see now this system as formed by three subsystems $S^{(j)}$, corresponding to a block of two consecutive stories of the building. Schematically, we write $S^{(1)}=[1, 2]$, $S^{(2)}=[2, 3]$, $S^{(3)}=[3, 4]$ (see Fig. 4). This decomposition defines a multi-overlapping decomposition with two overlapping blocks corresponding to stories 2 and 3. The state subsystem dimensions are $d_x^{(j)}=4$, $j=1, 2, 3$, with overlapping blocks of size $o_x^{(j)}=2$, $j=1, 2$. Regarding the inputs, the subsystem dimensions are $d_u^{(j)}=2$, $j=1, 2, 3$, with overlapping blocks of size $o_u^{(j)}=1$, $j=1, 2$.

Following the notation introduced in Subsection 2.3, we have $r=2$ overlapping blocks and we start with the pair $P_1^{(3)}=(A, B^{(a)})$. The numbers that define the first

expansion step (with index $j=2$) are

$$\begin{cases} n_1^{(2)} = \sum_{i=1}^2 (d_x^{(i)} - o_x^{(i)}) = 4 \\ n_2^{(2)} = o_x^{(2)} = 2 \\ n_3^{(2)} = d_x^{(3)} - o_x^{(2)} = 2 \\ m_1^{(2)} = \sum_{i=1}^2 (d_u^{(i)} - o_u^{(i)}) = 2 \\ m_2^{(2)} = o_u^{(2)} = 1 \quad m_3^{(2)} = d_u^{(3)} - o_u^{(2)} = 1. \end{cases} \quad (10)$$

Now, we proceed as described previously and use the expansion matrices $V^{(2)}$, $R^{(2)}$, defined by the numbers in (10), to compute the decoupled expanded pairs $P_1^{(2)}=(\tilde{A}_1^{(2)}, \tilde{B}_1^{(2)})$ and $P_2^{(2)}=(\tilde{A}_2^{(2)}, \tilde{B}_2^{(2)})$, where

$$\tilde{A}_1^{(2)} = 10^3 \times \begin{bmatrix} 0 & 0.0010 & 0 & 0 & 0 & 0 \\ -0.9850 & -0.0085 & 0.9850 & 0.0085 & 0 & 0 \\ 0 & 0 & 0 & 0.0010 & 0 & 0 \\ 0.9850 & 0.0085 & -1.9699 & -0.0170 & 0.9850 & 0.0085 \\ 0 & 0 & 0 & 0 & 0 & 0.0010 \\ 0 & 0 & 0.9850 & 0.0085 & -1.9699 & -0.0170 \end{bmatrix},$$

$$\tilde{B}_1^{(2)} = 10^{-5} \times \begin{bmatrix} 0 & 0 & 0 \\ -0.2894 & 0.2894 & 0 \\ 0 & 0 & 0 \\ 0.2894 & -0.5787 & 0.2894 \\ 0 & 0 & 0 \\ 0 & 0.2894 & -0.5787 \end{bmatrix}$$

and

$$\tilde{A}_2^{(3)} = 10^3 \times \begin{bmatrix} 0 & 0.0010 & 0 & 0 \\ -1.9699 & -0.0170 & 0.9850 & 0.0085 \\ 0 & 0 & 0 & 0.0010 \\ 0.9850 & 0.0085 & -1.9699 & -0.0170 \end{bmatrix},$$

$$\tilde{B}_2^{(3)} = 10^{-5} \times \begin{bmatrix} 0 & 0 \\ -0.5787 & 0.2894 \\ 0 & 0 \\ 0.2894 & -0.5787 \end{bmatrix}.$$

The pair $P_2^{(3)}=(\tilde{A}_2^{(3)}, \tilde{B}_2^{(3)})$ contains no overlapping blocks, and we choose the quadratic index

$$J_2^{(3)}(x(t), u(t)) = \int_0^\infty [x^T(t)[Q_2^{(3)}]^*x(t) + u^T(t)[R_2^{(3)}]^*u(t)] dt,$$

with weighting matrices $[Q_2^{(3)}]^*=I_{n^{(3)}}$ and $[R_2^{(3)}]^*=10^{-15} I_{n^{(3)} \times m^{(3)}}$, where $n^{(3)}=n_2^{(2)}+n_3^{(2)}$, $m^{(3)}=m_2^{(2)}+m_3^{(2)}$, to compute the expanded gain matrix

$$\tilde{K}_2^{(3)} = 10^7 \times \begin{bmatrix} -0.1466 & -2.8833 & 0 & -0.0005 \\ 0 & -0.0005 & -0.1466 & -2.8833 \end{bmatrix}.$$

The expanded pair $P_1^{(2)}=(\tilde{A}_1^{(2)}, \tilde{B}_1^{(2)})$ still contains overlapping blocks and it is supplied as the starting point for the next expansion step (with index $j=1$), which uses the numbers

$$\begin{cases} n_1^{(1)} = \sum_{i=1}^1 (d_x^{(i)} - o_x^{(i)}) = 2 \\ n_2^{(1)} = o_x^{(1)} = 2 \\ n_3^{(1)} = d_x^{(2)} - o_x^{(1)} = 2 \\ m_1^{(1)} = \sum_{i=1}^1 (d_u^{(i)} - o_u^{(i)}) = 1 \\ m_2^{(1)} = o_u^{(1)} = 1 \\ m_3^{(1)} = d_u^{(2)} - o_u^{(1)} = 1 \end{cases}$$

to define expansion matrices $V^{(1)}$, $R^{(1)}$ in order to produce a new set of decoupled expanded pairs $P_1^{(1)}=(\tilde{A}_1^{(1)}, \tilde{B}_1^{(1)})$ and $P_2^{(1)}=(\tilde{A}_2^{(1)}, \tilde{B}_2^{(1)})$. The pair

$P_2^{(2)} = (\tilde{A}_2^{(2)}, \tilde{B}_2^{(2)})$ contains no overlapping blocks and we use a quadratic index $J_2^{(2)}$ with weighting matrices $[Q_2^{(2)}]^* = I_{n^{(2)}}$ and $[R_2^{(2)}]^* = 10^{-15} I_{n^{(2)} \times m^{(2)}}$, where $n^{(2)} = n_2^{(1)} + n_3^{(1)}$, $m^{(2)} = m_2^{(1)} + m_3^{(1)}$, to compute the expanded gain matrix

$$\tilde{K}_2^{(2)} = 10^7 \times \begin{bmatrix} -0.1466 & -2.8833 & 0 & -0.0005 \\ 0 & -0.0005 & -0.1466 & -2.8833 \end{bmatrix}.$$

As we have completed the expansion process, the expanded pair $P_1^{(1)}$ also has no overlapping blocks. We select the quadratic index $J_1^{(1)}$ with weighting matrices $[Q_1^{(1)}]^* = I_{n^{(1)}}$ and $[R_1^{(1)}]^* = 10^{-15} I_{n^{(1)} \times m^{(2)}}$, $n^{(1)} = n_1^{(1)} + n_2^{(1)}$, $m^{(1)} = m_1^{(1)} + m_2^{(1)}$, and compute the expanded gain matrix

$$\tilde{K}_1^{(1)} = 10^7 \times \begin{bmatrix} -0.1466 & -2.8854 & 0 & -0.0016 \\ 0 & -0.0016 & -0.1466 & -2.8838 \end{bmatrix}.$$

The contraction process starts with the matrix $\tilde{K}^{(1)} = \text{diag}(\tilde{K}_1^{(1)}, \tilde{K}_2^{(2)})$, which is contracted to obtain the gain matrix

$$\tilde{K}_1^{(2)} = 10^7 \times \begin{bmatrix} -0.1466 & -2.8854 & 0 & -0.0016 & 0 & 0 \\ 0 & -0.0008 & -0.1466 & -2.8835 & 0 & -0.0003 \\ 0 & 0 & 0 & -0.0005 & -0.1466 & -2.8833 \end{bmatrix}.$$

In the second contraction step, the matrix $\tilde{K}^{(2)} = \text{diag}(\tilde{K}_1^{(2)}, \tilde{K}_2^{(3)})$ is contracted to obtain $\tilde{K}_1^{(3)}$, in Fig. 16. This last matrix is the desired multi-overlapping controller, denoted by $K_o^{(a)}$, which is given in Fig. 16.

Direct actuators. We consider now the main system $S^{(b)}$ defined by the pair $(A, B^{(b)})$. In this case, the previously described procedure yields the expanded gain matrices

$$\begin{aligned} \tilde{K}_1^{(1)} &= 10^7 \times \begin{bmatrix} 0.1463 & 2.5551 & -0.0003 & -1.1441 \\ 0.1459 & 1.4110 & 0.1463 & 2.5551 \end{bmatrix}, \\ \tilde{K}_2^{(2)} &= 10^7 \times \begin{bmatrix} 2.5977 & 2.2173 & 2.8431 & -1.2756 \\ -5.6100 & 1.2415 & 2.7594 & 2.5171 \end{bmatrix}, \\ \tilde{K}_2^{(3)} &= 10^7 \times \begin{bmatrix} 2.5977 & 2.2173 & 2.8431 & -1.2756 \\ -5.6100 & 1.2415 & 2.7594 & 2.5171 \end{bmatrix}. \end{aligned}$$

After completing the contraction process, the following multi-overlapping controller $K_o^{(b)}$ results, which given in Fig. 16.

3.4 Numerical simulations

In this section, the optimal LQR centralized state feedback controllers obtained in Subsection 3.2 are taken as a reference to assess the performance of the corresponding multi-overlapping controllers computed through the proposed sequential decomposition procedure. Firstly, for each one of the two considered actuation schemes, the suboptimal cost of the multi-overlapping controllers with respect to the centralized quadratic index J_c , defined in (9), is computed and compared with the corresponding optimal values. Secondly, numerical simulations of the free response and the controlled response of the system under a seismic excitation are carried out for all the considered controllers. The maximum absolute inter-story drifts, and the maximum absolute control actions are computed and pertinently compared. The

1940 El Centro NS earthquake (Fig. 6), scaled to a peak of $1m/s^2$, has been used as ground acceleration input in the simulations.

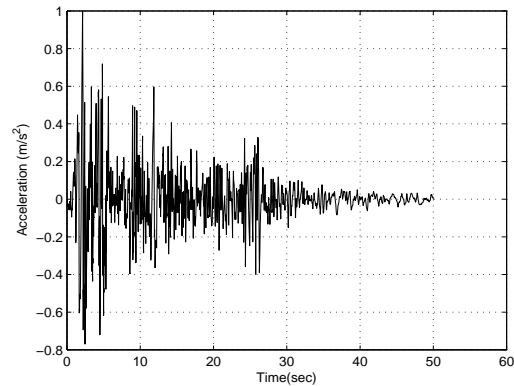


Fig. 6. El Centro NS earthquake, scaled to a peak of $1m/s^2$.

Inter-story actuators. In this case, the centralized optimal LQR gain matrix $K_c^{(a)}$ and the multi-overlapping gain $K_o^{(a)}$ are very similar (see Fig. 16). The quadratic index cost J_c associated to the controller $u(t) = K_o^{(a)} x(t)$, can be computed as $[J_c^{(a)}]_o = \text{trace}[P_o^{(a)}]$, where the matrix $P_o^{(a)}$ can be obtained using the Matlab command `lyap()` with arguments

$$A_{cl}^T = [A - B^{(a)} K_o^{(a)}]^T, \quad H = Q^* + [K_o^{(a)}]^T R^* K_o^{(a)}.$$

The resulting cost is $[J_c^{(a)}]_o = 38.58$, which is practically equal to the optimal cost. The upper plot in Fig. 7

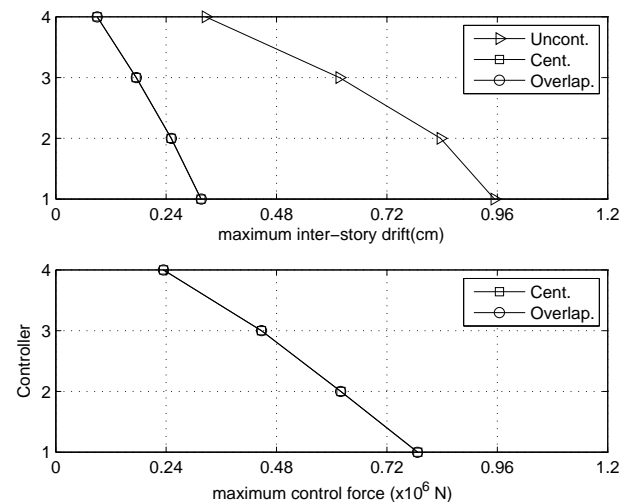


Fig. 7. Maximum inter-story drifts and control forces for inter-story actuators.

displays the maximum absolute inter-story drifts for the uncontrolled system, the optimal LQR centralized controller, and the multi-overlapping controller. In the lower

plot, the maximum absolute control efforts are shown. As may be expected from the small differences observed in the gain matrices, the behavior of the optimal LQR centralized controller and the multi-overlapping controller are practically equal. In fact, the corresponding graphs overlap and appear as a single line.

Direct actuators. In this second case, the centralized controller has an optimal cost $[J_c^{(b)}]_{opt} = 45.06$, while the multi-overlapping controller has a suboptimal cost $[J_c^{(a)}]_o = 46.99$. The corresponding gain matrices $K_c^{(b)}$, $K_o^{(b)}$ are given in Fig. 16. The maximum absolute inter-story drifts and maximum absolute control efforts are displayed in Fig. 8. It can be observed that, even in

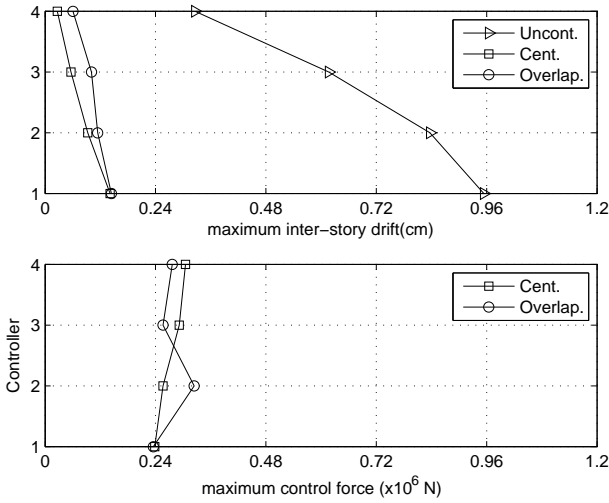


Fig. 8. Maximum inter-story drifts and control forces for direct actuators.

this case where the optimal centralized gain matrix is a full matrix, the multi-overlapping controller maintains a remarkably high level of performance.

4 OUTPUT-FEEDBACK CONTROL

In this section a new approach will be developed. This approach is based on the output-feedback control design by using H_∞ control, which can be useful when some state variables are not available for feedback purpose. A brief summary about the H_∞ control is offered in the next subsection.

4.1 Background results: H_∞ control design

In this subsection, theoretical LMI results to obtain output-feedback H_∞ controllers are presented. Consider a class of linear continuous-time systems described by the equations

$$\begin{aligned} \mathbf{S} : \dot{x}(t) &= Ax(t) + Bu(t) + Ew(t), \\ y(t) &= C_y x(t), \\ z(t) &= C_z x(t) + D_z u(t), \end{aligned} \quad (11)$$

where $x(t) \in \mathbb{R}^n$ corresponds to the state, $u(t) \in \mathbb{R}^m$ is the input control, $w(t) \in L_2^p[0, \infty)$ the disturbance input, $y(t) \in \mathbb{R}^l$ is the output and $z(t) \in \mathbb{R}^q$ the controlled output. A, B, E, C_y, C_z, D_z are known, real and constant matrices of appropriate dimensions.

Consider an output-feedback controller $u(t) = Ky(t)$ for the system (11), where $K \in \mathbb{R}^{m \times l}$. Then, the resulting closed-loop system has the form

$$\mathbf{S}_C : \begin{aligned} \dot{x}(t) &= [A + BKC_y]x(t) + Ew(t), \\ z(t) &= [C_z + D_zKC_y]x(t). \end{aligned} \quad (12)$$

The objective is to design an output-feedback controller $u(t) = Ky(t)$ satisfying two requirements: (i) the closed-loop system (12) is asymptotically stable when $w(t) = 0$; and (ii) it guarantees a prescribed H_∞ -norm disturbance attenuation of the closed-loop system from $w(t)$ to $z(t)$, i.e.

$$\|z(t)\|_2 \leq \gamma \|w(t)\|_2, \quad \gamma > 0,$$

for all nonzero $w(t) \in L_2^p[0, \infty)$ and zero initial conditions, with a minimum γ value.

Having this idea in mind, let us introduce the following index:

$$\begin{aligned} J &= \int_0^\infty [z^T(t)z(t) - \gamma^2 w^T(t)w(t)] dt \\ &= \|z(t)\|_2^2 - \gamma^2 \|w(t)\|_2^2, \end{aligned}$$

under zero initial conditions. Consider the closed-loop system given in (12). For any $w(t) \neq 0$ such that $w(t) \in L_2^p[0, \infty)$, we have

$$J \leq \int_0^\infty [z^T(t)z(t) - \gamma^2 w^T(t)w(t) + \dot{V}(x, t)] dt, \quad (13)$$

where $V(x, t) = x^T(t)Px(t)$ is a Lyapunov function with P a symmetric positive-definite matrix. Substituting $z(t)$ and $\dot{V}(x, t)$ into (13), we obtain

$$J \leq \int_0^\infty x^T(t) [S + [C_z + D_zKC_y]^T [C_z + D_zKC_y]] x(t) dt, \quad (14)$$

where

$$S = PA + [PA]^T + PBKC_y + [PBKC_y]^T + \gamma^{-2} PEE^T P.$$

The inequality (14) can be transformed into an LMI problem by introducing the change of variables $X = P^{-1}$, $W = KC_y X$, and $\eta = \gamma^{-2}$ (see [23]). Then, the following theorem can be stated.

Theorem 2: Consider a linear continuous-time system given in (11). For a prescribed scalar $\eta > 0$, suppose that there exists a matrix $X > 0$ and a matrix W such that the following linear matrix inequality

$$\begin{bmatrix} W_1 & W_2^T \\ W_2 & -I \end{bmatrix} < 0 \quad (15)$$

holds, where

$$\begin{aligned} W_1 &= AX + [AX]^T + BW + [BW]^T + \eta EE^T, \\ W_2 &= C_z X + D_z W. \end{aligned}$$

Then, $u(t)=Ky(t)$ is an output-feedback controller such that the resulting closed-loop system (12) is asymptotically stable with H_∞ bounded norm γ .

Now, the output-feedback H_∞ control problem can be transformed into the following convex optimization problem:

$$\begin{cases} \text{maximize } \eta \\ \text{subject to } X > 0, \eta > 0 \text{ and the LMI (15).} \end{cases} \quad (16)$$

4.2 Output-feedback control design

From Theorem 2, in order to obtain an output-feedback-controller $u(t)=Ky(t)$ for the system \mathbf{S} , it is necessary to isolate the gain matrix K . To solve this problem, the following procedure can be used [30]:

Step 1) Select a full rank $n \times (n - q)$ dimensional matrix Q such that $C_y Q = 0$. The matrix Q may be taken as C_y^\perp , for example choosing the columns of Q to be a basis of the orthogonal space of $\mathcal{R}(C_y)$, that is, the space generated by the rows of C_y .

Step 2) Solve the problem stated in (15) with

$$\begin{aligned} X &= QX_qQ^T + C_y^T [C_y C_y^T]^{-1} C_y + C_y^T X_c C_y, \\ Y &= Y_c C_y, \end{aligned}$$

where X_q and X_c are unknown symmetric matrices of $(n-q) \times (n-q)$ and $q \times q$ dimensions, respectively, and Y_c is an unknown $m \times q$ dimensional matrix.

Step 3) Compute the gain matrix K as

$$K = Y_c \left[I - C_y X_0^{-1} C_y^T X_c [I + C_y X_0^{-1} C_y^T X_c]^{-1} \right],$$

where $X_0 = QX_qQ^T + C_y^T [C_y C_y^T]^{-1} C_y$. This procedure guarantees $KC_y = YX^{-1}$ and, furthermore, the matrix K has been isolated.

5 EXAMPLE: FIVE-STORY BUILDING MODEL

A simplified one-dimensional model of a five-story building has been selected. The control goal is to reduce the inter-story drifts when the building is subjected to a ground excitation (see Fig. 9). The building motion can

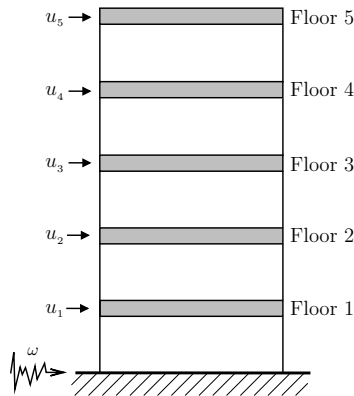


Fig. 9. Actuation scheme for a five-story building.

be described by

$$\mathbf{M}\ddot{q}(t) + \mathbf{C}\dot{q}(t) + \mathbf{K}q(t) = \mathbf{T}_u u(t) + \mathbf{T}_w w(t), \quad (17)$$

where $q(t) \in \mathbb{R}^5$ is the displacement vector relative to the ground and \mathbf{M} , \mathbf{C} , \mathbf{K} , are the mass, damping, and stiffness matrices, respectively. The vector $u(t) \in \mathbb{R}^5$ is the control force, $w(t) \in \mathbb{R}$ is the ground acceleration, \mathbf{T}_w is the excitation location matrix, and \mathbf{T}_u is the control location matrix. The particular values of the matrices are the following:

$$\mathbf{M} = 10^2 \times \text{diag} [3456, 3456, 3456, 3456, 3456],$$

$$\mathbf{C} = \begin{bmatrix} 5874 & -2937 & 0 & 0 & 0 \\ -2937 & 5874 & -2937 & 0 & 0 \\ 0 & -2937 & 5874 & -2937 & 0 \\ 0 & 0 & -2937 & 5874 & -2937 \\ 0 & 0 & 0 & -2937 & 2937 \end{bmatrix},$$

$$\mathbf{K} = 10^2 \times \begin{bmatrix} 6808 & -3404 & 0 & 0 & 0 \\ -3404 & 6808 & -3404 & 0 & 0 \\ 0 & -3404 & 6808 & -3404 & 0 \\ 0 & 0 & -3404 & 6808 & -3404 \\ 0 & 0 & 0 & -3404 & 3404 \end{bmatrix},$$

$$\mathbf{T}_u = \text{diag} [1, 1, 1, 1, 1],$$

$$\mathbf{T}_w = -\mathbf{M}[1, 1, 1, 1, 1]^T$$

where masses are in kg , damping coefficients are in $kN \cdot s/m$, and stiffness coefficients are in kN/m . From the second-order model (17), a first-order state-space model in the form given in (11) can be derived where the state vector $x(t) \in \mathbb{R}^{10}$ contains the inter-story drifts and velocities arranged in increasing order, that is,

$$x(t) = [q_1, \dot{q}_1, (q_2 - q_1), (\dot{q}_2 - \dot{q}_1), \dots, (q_5 - q_4), (\dot{q}_5 - \dot{q}_4)]^T.$$

A detailed derivation of the first-order state-space model can be found in [27]. For the particular values presented in (11), the state, the control and the input matrices A , B , and E are summarized in Fig. 16. The numerical values of the matrices C_y , C_z , and D_z given in (11) will be selected for each specific type of controller in the next subsection.

5.1 Numerical simulations

In this subsection, numerical simulations of the free and controlled responses of the system under a seismic excitation are carried out. The maximum absolute inter-story drifts and the maximum absolute control actions are computed and compared. The 1940 El Centro NS earthquake, scaled to a peak of $1m/s^2$, is used as ground acceleration input in the simulations (see Fig. 6).

Three different controllers have been considered. Firstly, the building is considered as a whole and a *centralized full-state H_∞ controller* is computed. This centralized controller will later be taken as a reference to assess the performance of the proposed static output-feedback controllers: a *partial output-feedback controller* and a *partial output-feedback overlapping controller*. For the overlapping controller, the building is seen as made up of two overlapped subsystems, which are composed by two blocks of stories: $\mathbf{S}_1 = [1, 2, 3]$ and $\mathbf{S}_2 = [3, 4, 5]$. In this case, the 3th story is the overlapped part.

a) Full-state control design

In order to compute a centralized controller, we consider $C_y=I_{10}$, $C_z=10 \times \begin{bmatrix} I_{10} \\ 0_{5 \times 10} \end{bmatrix}$ and $D_z=10^{-12} \times \begin{bmatrix} 0_{10 \times 5} \\ I_5 \end{bmatrix}$ given in (11). It can be observed that the matrix C_y corresponds to all the inter-story drifts and velocities. The computed full-state centralized gain matrix K_{full} is given in Fig. 16.

b) Partial output-feedback control design

We focus now our attention in designing a partial output-feedback controller. The matrices C_z and D_z are the same as given to compute a centralized controller. However, we suppose that the matrix C_y provides all the inter-story drifts, but only the inter-story velocities of the 1st and 3th stories. That is,

$$C_y = \begin{bmatrix} 1 & 0 & 0 & 0 & 0 & 0 & 0 & 0 & 0 & 0 & 0 \\ 0 & 1 & 0 & 0 & 0 & 0 & 0 & 0 & 0 & 0 & 0 \\ 0 & 0 & 1 & 0 & 0 & 0 & 0 & 0 & 0 & 0 & 0 \\ 0 & 0 & 0 & 0 & 1 & 0 & 0 & 0 & 0 & 0 & 0 \\ 0 & 0 & 0 & 0 & 0 & 1 & 0 & 0 & 0 & 0 & 0 \\ 0 & 0 & 0 & 0 & 0 & 0 & 1 & 0 & 0 & 0 & 0 \\ 0 & 0 & 0 & 0 & 0 & 0 & 0 & 1 & 0 & 0 & 0 \\ 0 & 0 & 0 & 0 & 0 & 0 & 0 & 0 & 1 & 0 & 0 \\ 0 & 0 & 0 & 0 & 0 & 0 & 0 & 0 & 0 & 1 & 0 \\ 0 & 0 & 0 & 0 & 0 & 0 & 0 & 0 & 0 & 0 & 1 \end{bmatrix}$$

Remark 2: We had unsuccessfully attempted to solve this kind of problem before, the main difficulty was that the associated LMI (15) resulted to be infeasible. Recently, we found that, in some cases, the infeasibility can be overcome by adding a small perturbation matrix ΔA to the state matrix A . In the present example, the perturbation matrix has been chosen as $\Delta A=-0.02 \times I_{10}$. It should be noted that the dynamic characteristics of the original and the perturbed system, with state matrix $A_p=(A+\Delta A)$, are very similar. Consequently, the perturbed state matrix A_p can be successfully used to design a static output controller for the original system.

The gain matrix K_{part} , corresponding to the partial output-feedback controller, is presented in Fig. 16.

c) Overlapping output-feedback control design

Now, we consider two subsystems $S_1=[1, 2, 3]$ and $S_2=[3, 4, 5]$ with an overlapping part in the 3th story (see Fig. 10). In this case, the matrix $(\tilde{C}_y)_{11}$ for the decoupled expanded system $\tilde{S}_D^{(1)}$ in (5), gives the inter-story drifts of the 1st, 2nd, and 3th stories, together with the 1st and 3th inter-story velocities.

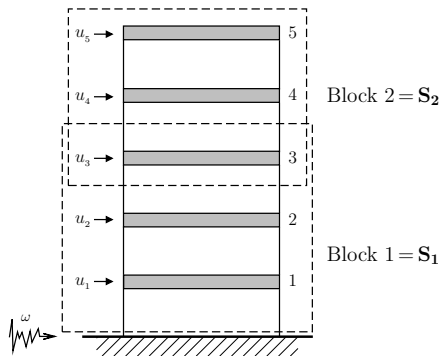


Fig. 10. Two-subsystem overlapping decomposition.

Analogously, the matrix $(\tilde{C}_y)_{22}$ for the decoupled expanded system $\tilde{S}_D^{(2)}$ provides the 3th, 4th, and 5th inter-story drifts, and only the 3th inter-story velocity. Thus,

$$(\tilde{C}_y)_{11} = \begin{bmatrix} 1 & 0 & 0 & 0 & 0 & 0 \\ 0 & 1 & 0 & 0 & 0 & 0 \\ 0 & 0 & 1 & 0 & 0 & 0 \\ 0 & 0 & 0 & 1 & 0 & 0 \\ 0 & 0 & 0 & 0 & 1 & 0 \\ 0 & 0 & 0 & 0 & 0 & 1 \end{bmatrix}, \quad (\tilde{C}_y)_{22} = \begin{bmatrix} 1 & 0 & 0 & 0 & 0 \\ 0 & 1 & 0 & 0 & 0 \\ 0 & 0 & 1 & 0 & 0 \\ 0 & 0 & 0 & 1 & 0 \\ 0 & 0 & 0 & 0 & 1 \end{bmatrix}$$

For the decoupled subsystems $\tilde{S}_D^{(1)}$, $\tilde{S}_D^{(2)}$, we consider the matrices $C_z=10 \times \begin{bmatrix} I_6 \\ 0_{3 \times 6} \end{bmatrix}$, $D_z=10^{-11.7} \times \begin{bmatrix} 0_{6 \times 3} \\ I_3 \end{bmatrix}$ and $C_z=10 \times \begin{bmatrix} I_6 \\ 0_{3 \times 6} \end{bmatrix}$, $D_z=10^{-13} \times \begin{bmatrix} 0_{6 \times 3} \\ I_3 \end{bmatrix}$, respectively. With the purpose to obtain feasibility of the corresponding local LMI problems, a perturbation matrix in the form $\Delta A=-0.02 \times I_6$ is added to the expanded state matrices \tilde{A}_{11} , \tilde{A}_{22} given in (5). Finally, the computed gain matrix for the overlapping output-feedback control K_{over} is offered in Fig. 16.

Seismic responses

In Figure 11, the maximum absolute inter-story drifts for the free (uncontrolled) system, the full-state controller, the partial output-feedback centralized controller and the overlapping output-feedback controller are displayed. The maximum absolute control efforts, for the same controllers, are shown in Fig. 12.

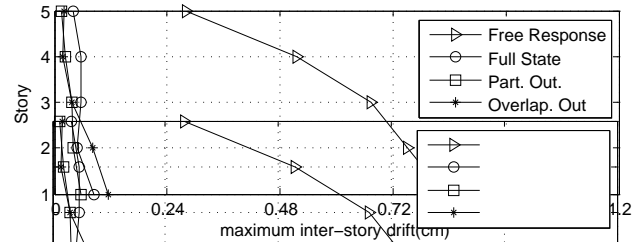


Fig. 11. Maximum inter-story drifts.

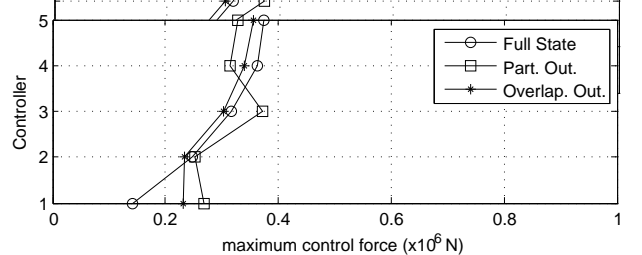


Fig. 12. Maximum control forces.

It can be observed that, despite the lower number of sensors and the reduced amount of information exchange, the partial output-feedback controller and the overlapping controller maintain a remarkably high level of performance when compared with the full-state centralized control. Comparing the two output controllers, the obtained results also illustrate the fact that suitable decentralized design strategies may be used to produce

controllers with a level of performance similar to their centralized counterparts.

6 MULTI-BUILDING CONNECTED SYSTEMS

In this section, we will focus our attention on the control of multi-building systems which, at the same time, can be high-rise buildings.

6.1 Two-building model

A simplified model for a two-building coupled system formed by a three-story building and a two-story building, linked by viscoelastic dampers, is presented. The buildings motion can be described by

$$\mathbf{M}\ddot{q}(t) + \mathbf{C}\dot{q}(t) + \mathbf{K}q(t) = \mathbf{T}_u u(t) + \mathbf{T}_w w(t). \quad (18)$$

The vector of relative displacements, with respect to the ground, is

$$q(t) = [q_1^{(l)}(t), q_2^{(l)}(t), q_3^{(l)}(t), q_1^{(r)}(t), q_2^{(r)}(t)]^T,$$

where $q_i^{(l)}(t)$ and $q_i^{(r)}(t)$ represent the displacement of the i th story in the left and right building, respectively. The vector of control forces has a similar structure

$$u(t) = [u_1^{(l)}(t), u_2^{(l)}(t), u_3^{(l)}(t), u_1^{(r)}(t), u_2^{(r)}(t)]^T,$$

where $\mathbf{T}_u = I_{5 \times 5}$ is the control location matrix, $\mathbf{T}_w = -\mathbf{M}[1, \dots, 1]^T$ is the excitation location matrix, and $w(t)$ is the ground acceleration. With the notations indicated in Fig. 13, the matrices in equation (18) have

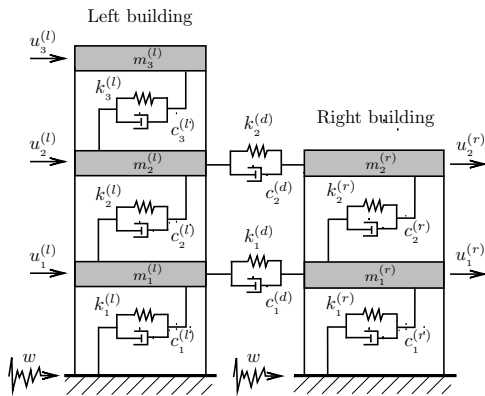


Fig. 13. Structural model for two adjacent buildings

the following structures:

$$\mathbf{M} = \begin{bmatrix} \mathbf{M}_L & \mathbf{0} \\ \mathbf{0} & \mathbf{M}_R \end{bmatrix},$$

$$\mathbf{M}_L = \text{diag} [m_1^{(l)}, m_2^{(l)}, m_3^{(l)}], \quad \mathbf{M}_R = \text{diag} [m_1^{(r)}, m_2^{(r)}],$$

$$\mathbf{C} = \mathbf{C}^s + \mathbf{C}^d, \quad \mathbf{K} = \mathbf{K}^s + \mathbf{K}^d.$$

The inter-story damping matrix is

$$\mathbf{C}^s = \begin{bmatrix} \mathbf{C}_L & \mathbf{0} \\ \mathbf{0} & \mathbf{C}_R \end{bmatrix},$$

with

$$\mathbf{C}_L = \begin{bmatrix} c_1^{(l)} + c_2^{(l)} & -c_2^{(l)} & 0 \\ -c_2^{(l)} & c_2^{(l)} + c_3^{(l)} & -c_3^{(l)} \\ 0 & -c_3^{(l)} & c_3^{(l)} \end{bmatrix}, \quad \mathbf{C}_R = \begin{bmatrix} c_1^{(r)} + c_2^{(r)} & -c_2^{(r)} \\ -c_2^{(r)} & c_2^{(r)} \end{bmatrix},$$

while the inter-building damping matrix corresponding to the viscoelastic dampers is

$$\mathbf{C}^d = \begin{bmatrix} c_1^{(d)} & 0 & 0 & -c_1^{(d)} & 0 \\ 0 & c_2^{(d)} & 0 & 0 & -c_2^{(d)} \\ 0 & 0 & 0 & 0 & 0 \\ -c_1^{(d)} & 0 & 0 & c_1^{(d)} & 0 \\ 0 & -c_2^{(d)} & 0 & 0 & c_2^{(d)} \end{bmatrix}.$$

Analogously, the inter-story stiffness matrix is

$$\mathbf{K}^s = \begin{bmatrix} \mathbf{K}_L & \mathbf{0} \\ \mathbf{0} & \mathbf{K}_R \end{bmatrix},$$

with

$$\mathbf{K}_L = \begin{bmatrix} k_1^{(l)} + k_2^{(l)} & -k_2^{(l)} & 0 \\ -k_2^{(l)} & k_2^{(l)} + k_3^{(l)} & -k_3^{(l)} \\ 0 & -k_3^{(l)} & k_3^{(l)} \end{bmatrix}, \quad \mathbf{K}_R = \begin{bmatrix} k_1^{(r)} + k_2^{(r)} & -k_2^{(r)} \\ -k_2^{(r)} & k_2^{(r)} \end{bmatrix},$$

and the inter-building stiffness matrix takes the form

$$\mathbf{K}^d = \begin{bmatrix} k_1^{(d)} & 0 & 0 & -k_1^{(d)} & 0 \\ 0 & k_2^{(d)} & 0 & 0 & -k_2^{(d)} \\ 0 & 0 & 0 & 0 & 0 \\ -k_1^{(d)} & 0 & 0 & k_1^{(d)} & 0 \\ 0 & -k_2^{(d)} & 0 & 0 & k_2^{(d)} \end{bmatrix}.$$

From the second-order model (18), a first-order state-space model can be derived

$$\mathcal{S} : \begin{cases} \dot{x}(t) = Ax(t) + Bu(t) + Ew(t), \\ y(t) = Cyx(t). \end{cases} \quad (19)$$

Here, the state vector $x(t) \in \mathbb{R}^{10}$ groups together the displacements and the velocities arranged in increasing order, that is,

$$x(t) = [q_1(t), \dot{q}_1(t), \dots, q_5(t), \dot{q}_5(t)]^T,$$

where $q_i(t) = q_i^{(l)}(t)$, $i=1, 2, 3$, is the displacement relative to the ground of the i th story in the left building, and $q_4(t) = q_1^{(r)}(t)$, $q_5(t) = q_2^{(r)}(t)$ denote the displacements for the right building. The matrices for the state-space model (19) used in the controllers design and the response

numerical simulations are

$$A = \begin{bmatrix} 0 & 1 & 0 & 0 & 0 & 0 & 0 & 0 & 0 & 0 \\ -6201 & -0.2 & 3100 & 0.1 & 0 & 0 & 0 & 0 & 0 & 0 \\ 0 & 0 & 0 & 1 & 0 & 0 & 0 & 0 & 0 & 0 \\ 3100 & 0.1 & -6201 & -0.9 & 3100 & 0.1 & 0 & 0 & 0 & 0.8 \\ 0 & 0 & 0 & 0 & 0 & 1 & 0 & 0 & 0 & 0 \\ 0 & 0 & 3100 & 0.1 & -3100 & -0.1 & 0 & 0 & 0 & 0 \\ 0 & 0 & 0 & 0 & 0 & 0 & 1 & 0 & 0 & 0 \\ 0 & 0 & 0 & 0 & 0 & 0 & 0 & 1 & 0 & 0 \\ 0 & 0 & 0 & 0 & 0 & 0 & -3100 & -0.2 & 1550 & 0.1 \\ 0 & 0 & 0 & 0 & 0 & 0 & 0 & 0 & 0 & 1 \\ 0 & 0 & 0 & 0.8 & 0 & 0 & 1550 & 0.1 & -1550 & -0.9 \end{bmatrix},$$

$$B = 10^{-6} \times \begin{bmatrix} 0 & 0 & 0 & 0 & 0 & 0 & 0 & 0 & 0 & 0 \\ 0.7752 & 0 & 0 & 0 & 0 & 0 & 0 & 0 & 0 & 0 \\ 0 & 0 & 0 & 0 & 0 & 0 & 0 & 0 & 0 & 0 \\ 0 & 0.7752 & 0 & 0 & 0 & 0 & 0 & 0 & 0 & 0 \\ 0 & 0 & 0 & 0 & 0 & 0 & 0 & 0 & 0 & 0 \\ 0 & 0 & 0.7752 & 0 & 0 & 0 & 0 & 0 & 0 & 0 \\ 0 & 0 & 0 & 0 & 0 & 0 & 0 & 0 & 0 & 0 \\ 0 & 0 & 0 & 0 & 0.7752 & 0 & 0 & 0 & 0 & 0 \\ 0 & 0 & 0 & 0 & 0 & 0 & 0.7752 & 0 & 0 & 0 \\ 0 & 0 & 0 & 0 & 0 & 0 & 0 & 0 & 0 & 0 \\ 0 & 0 & 0 & 0 & 0 & 0 & 0 & 0.7752 & 0 & 0 \end{bmatrix},$$

$$E = [0, -1, 0, -1, 0, -1, 0, -1, 0, -1]^T,$$

$$C_y = \begin{bmatrix} 1 & 0 & 0 & 0 & 0 & 0 & 0 & 0 & 0 & 0 \\ -1 & 0 & 1 & 0 & 0 & 0 & 0 & 0 & 0 & 0 \\ 0 & 0 & -1 & 0 & 1 & 0 & 0 & 0 & 0 & 0 \\ 0 & 0 & 0 & 0 & 0 & 0 & 1 & 0 & 0 & 0 \\ 0 & 0 & 0 & 0 & 0 & 0 & -1 & 0 & 1 & 0 \end{bmatrix}.$$

(20)

It should be noted that the output matrix C_y extracts the inter-story drifts of the buildings, that is,

$$y(t) = [y_1^{(l)}(t), y_2^{(l)}(t), y_3^{(l)}(t), y_1^{(r)}(t), y_2^{(r)}(t)]^T,$$

where $y_1^{(l)} = q_1^{(l)}$, $y_2^{(l)} = q_2^{(l)} - q_1^{(l)}$, $y_3^{(l)} = q_3^{(l)} - q_2^{(l)}$, $y_1^{(r)} = q_1^{(r)}$, $y_2^{(r)} = q_2^{(r)} - q_1^{(r)}$. The matrices in (20) correspond to the following particular values of the mass, damping and stiffness coefficients: $m_i^{(l)} = m_j^{(r)} = 1.29 \times 10^6 \text{ Kg}$; $c_i^{(l)} = c_j^{(r)} = 10^5 \text{ N}\cdot\text{s/m}$; $k_i^{(l)} = 4 \times 10^9 \text{ N}\cdot\text{s/m}$; $k_j^{(r)} = 2 \times 10^9 \text{ N}\cdot\text{s/m}$; $c_1^{(d)} = 0$, $c_2^{(d)} = 10^6 \text{ N}\cdot\text{s/m}$; $k_j^{(d)} = 0$, for $i=1, 2, 3, j=1, 2$. A detailed derivation of the first-order state-space model (19) can be found in [27].

6.2 Controllers design

In this subsection, three active H_∞ controllers for the system (19) are computed: a *centralized controller* and two *decentralized controllers*; in all the cases, the particular values given in (20) are used. The centralized controller will be taken as a reference in the performance assessment. For the decentralized controllers, two different approaches are followed: a centralized design which uses the overall two-building coupled model, and a decentralized design which considers the buildings independently, ignoring the linkage. Regarding to the passive control system, the buildings are linked by a single damper with damping constant $c_2^{(d)} = 10^6 \text{ N}\cdot\text{s/m}$, located at the second story. This configuration may be considered as optimal, in the sense that numerical simulations show that no significant reduction of the vibrational response results when a similar damper is placed linking the first stories, or elastic linking elements are considered. In terms of the damping and stiffness coefficients, this means $c_1^{(d)} = 0$, $k_1^{(d)} = k_2^{(d)} = 0$. Finally, a number of good reasons justify the choice of the H_∞ approach for the problem under consideration: the practical interpretation of the H_∞ norm as minimum worst case gain from energy disturbance to energy response, the

existence of efficient solvers via LMI formulation which allow to obtain decentralized controllers by imposing structure constraints on the controller gain matrix, and the possibility of extending the study to a variety of interesting scenarios which may include several kinds of uncertainties, delays, actuator saturation, etc.

a) H_∞ control design

Let us consider the system (19) together with the controlled output $z(t) = C_z x(t) + D_z u(t)$ (see [6]). For a given state feedback controller $u(t) = Gx(t)$, the following closed-loop system results

$$\mathcal{S}_{CL} : \begin{cases} \dot{x}(t) = A_{CL} x(t) + Ew(t), \\ z(t) = C_{CL} x(t), \end{cases}$$

where

$$A_{CL} = A + BG, \quad C_{CL} = C_z + D_z G. \quad (21)$$

The closed-loop transfer function from the disturbance $w(t)$ to the controlled output $z(t)$ has the form

$$T_{zw}(s) = C_{CL} (sI - A_{CL})^{-1} E. \quad (22)$$

The objective is to find a gain matrix G_{op} which produces a stable matrix A_{CL} and, at the same time, minimizes the value of the norm

$$\|T_{zw}\|_\infty = \max_{\omega} \bar{\sigma} [T_{zw}(j\omega)], \quad (23)$$

where $\bar{\sigma}(\cdot)$ denotes the maximum singular value. For a prescribed $\gamma > 0$, according to the Bounded Real Lemma, the following two statements are equivalent:

- 1) $\|T_{zw}\|_\infty < \gamma$ and A_{CL} is stable.
- 2) There exists a symmetric positive-definite matrix $P \in \mathbb{R}^{2n \times 2n}$ such that the following inequality

$$\begin{bmatrix} A_{CL} P + P A_{CL}^T + \gamma^{-2} E E^T & P C_{CL}^T \\ * & -I \end{bmatrix} < 0$$

holds, where $*$ denotes the symmetric entry.

By using the closed-loop matrix definitions given in (21), the inequations given by the Bounded Real Lemma becomes

$$\begin{bmatrix} AP + P A^T + BGP + P G^T B^T + \gamma^{-2} E E^T & P C_z^T + P G^T D_z^T \\ * & -I \end{bmatrix} < 0.$$

The above nonlinear matrix inequality can be converted into a linear matrix inequality (LMI) by introducing the new variables $Y = GP$ and $\eta = \gamma^{-2}$

$$\begin{bmatrix} AP + P A^T + B Y + Y^T B^T + \eta E E^T & P C_z^T + Y^T D_z^T \\ * & -I \end{bmatrix} < 0. \quad (24)$$

The continuous-time H_∞ control problem is then transformed into the following convex optimization problem:

$$\begin{cases} \text{maximize } \eta \\ \text{subject to } P > 0, \eta > 0 \text{ and the LMI (24),} \end{cases} \quad (25)$$

where the matrices Y, P are the optimization variables. If the optimal value η_{\max} is attained for the optimal

matrices Y_{op} , P_{op} , the corresponding gain matrix can be computed as

$$G_{op} = Y_{op} P_{op}^{-1},$$

and the value of the minimum H_∞ norm is

$$\|T_{zw}(G_{op})\|_\infty = \gamma_{G_{op}} = \frac{1}{\sqrt{\eta_{\max}}},$$

where $T_{zw}(G_{op})$ denotes the transfer function described in (22) corresponding to the control gain matrix G_{op} .

b) Centralized control

First, we compute a centralized H_∞ control by solving the optimization problem stated in (25) using the system matrices given in (20) and the controlled output matrices

$$C_z = \begin{bmatrix} C_y \\ 0_{5 \times 10} \end{bmatrix}, \quad D_z = 0.3162 \times 10^{-7} \begin{bmatrix} 0_{5 \times 5} \\ I_{5 \times 5} \end{bmatrix},$$

obtaining the following full control gain matrix

$$G_c = 10^7 \times$$

$$\begin{bmatrix} 0.133 & -0.061 & 0.180 & -0.082 & 0.289 & -0.083 & -0.810 & -0.031 & -1.422 & -0.050 \\ 0.275 & -0.082 & 0.344 & -0.145 & 0.498 & -0.165 & -1.515 & -0.055 & -2.527 & -0.091 \\ 0.302 & -0.083 & 0.470 & -0.165 & 0.594 & -0.226 & -1.992 & -0.070 & -3.071 & -0.113 \\ 0.711 & -0.031 & 1.300 & -0.057 & 1.687 & -0.070 & -0.254 & -0.072 & -0.445 & -0.067 \\ 1.231 & -0.050 & 2.227 & -0.091 & 2.573 & -0.113 & -0.336 & -0.067 & -0.736 & -0.138 \end{bmatrix}$$

and the minimum γ value

$$\|T_{zw}(G_c)\|_\infty = \gamma_{G_c} = 0.0788.$$

Note that to compute the actuation force for any story using the gain matrix G_c , the knowledge of the complete state of both buildings is required.

c) Decentralized control with centralized design

Second, we consider again the overall two-building coupled system but now the goal is to design a decentralized controller by imposing a block diagonal structure on the control gain matrix. To this end, we solve problem (25) using variable matrices P and Y with the form

$$P = \begin{bmatrix} P_{11} & 0 \\ 0 & P_{22} \end{bmatrix}, \quad Y = \begin{bmatrix} Y_{11} & 0 \\ 0 & Y_{22} \end{bmatrix},$$

where P_{11} , P_{22} are positive-definite matrices of dimensions 6×6 and 4×4 , respectively, and Y_{11} , Y_{22} are rectangular matrices of dimensions 3×6 and 2×4 . The matrices used in the controlled output $z(t) = C_z x(t) + D_z u(t)$ are

$$C_z = \begin{bmatrix} C_y \\ 0_{5 \times 10} \end{bmatrix}, \quad D_z = 0.5623 \times 10^{-7} \begin{bmatrix} 0_{5 \times 5} \\ I_{5 \times 5} \end{bmatrix}.$$

After solving the corresponding constrained LMI minimization problem, the following block diagonal gain matrix results

$$G_{dc} = 10^6 \times$$

$$\begin{bmatrix} 0.078 & -1.049 & 0.094 & -1.177 & -0.230 & -1.426 & 0 & 0 & 0 & 0 \\ 0.320 & -1.177 & 0.056 & -2.476 & -0.268 & -2.603 & 0 & 0 & 0 & 0 \\ 0.497 & -1.426 & 0.190 & -2.603 & -0.346 & -3.653 & 0 & 0 & 0 & 0 \\ 0 & 0 & 0 & 0 & 0 & 0 & 0.057 & -1.220 & -0.153 & -1.346 \\ 0 & 0 & 0 & 0 & 0 & 0 & 0.354 & -1.346 & -0.269 & -2.566 \end{bmatrix}$$

and the associated minimum γ value is

$$\|T_{zw}(G_{dc})\|_\infty = \gamma_{G_{dc}} = 0.1544.$$

In this case, we only need the state of the corresponding building to compute the actuation force for a given story. Predictably, a higher γ value has been obtained due to the structural restrictions imposed on matrices Y and P . However, the resulting γ value is still remarkably low.

d) Decentralized control with decentralized design

Finally, we proceed to design a decentralized controller considering the buildings independently and ignoring the passive linking system. In this third case, we have two independent subsystems

$$\mathcal{S}_L : \begin{cases} \dot{x}_L(t) = A_L x_L(t) + B_L u_L(t) + E_L w(t), \\ y_L(t) = (C_y)_L x_L(t), \end{cases} \quad (26)$$

$$\mathcal{S}_R : \begin{cases} \dot{x}_R(t) = A_R x_R(t) + B_R u_R(t) + E_R w(t), \\ y_R(t) = (C_y)_R x_R(t), \end{cases} \quad (27)$$

with state vectors

$$x_L(t) = \begin{bmatrix} q_1^{(l)}(t), \dot{q}_1^{(l)}(t), q_2^{(l)}(t), \dot{q}_2^{(l)}(t), q_3^{(l)}(t), \dot{q}_3^{(l)}(t) \end{bmatrix}^T, \\ x_R(t) = \begin{bmatrix} q_1^{(r)}(t), \dot{q}_1^{(r)}(t), q_2^{(r)}(t), \dot{q}_2^{(r)}(t) \end{bmatrix}^T,$$

control forces

$$u_L(t) = \begin{bmatrix} u_1^{(l)}(t), u_2^{(l)}(t), u_3^{(l)}(t) \end{bmatrix}^T, \quad u_R(t) = \begin{bmatrix} u_1^{(r)}(t), u_2^{(r)}(t) \end{bmatrix}^T,$$

and outputs

$$y_L(t) = \begin{bmatrix} y_1^{(l)}(t), y_2^{(l)}(t), y_3^{(l)}(t) \end{bmatrix}^T, \quad y_R(t) = \begin{bmatrix} y_1^{(r)}(t), y_2^{(r)}(t) \end{bmatrix}^T.$$

The matrices in (26) and (27) can be easily derived from the matrices and values given in Subsection 6.1. For instance, the output matrices are

$$(C_y)_L = \begin{bmatrix} 1 & 0 & 0 & 0 & 0 & 0 \\ -1 & 0 & 1 & 0 & 0 & 0 \\ 0 & 0 & -1 & 0 & 1 & 0 \end{bmatrix}, \quad (C_y)_R = \begin{bmatrix} 1 & 0 & 0 & 0 \\ -1 & 0 & 1 & 0 \end{bmatrix}.$$

For the left subsystem \mathcal{S}_L , we consider the controlled output

$$z_L(t) = (C_z)_L x_L(t) + (D_z)_L u_L(t)$$

with

$$(C_z)_L = \begin{bmatrix} (C_y)_L \\ 0_{3 \times 6} \end{bmatrix}, \quad (D_z)_L = 0.5623 \times 10^{-7} \begin{bmatrix} 0_{3 \times 3} \\ I_{3 \times 3} \end{bmatrix},$$

to compute an H_∞ controller G_L . Analogously, for the right subsystem \mathcal{S}_R we take

$$z_R(t) = (C_z)_R x_R(t) + (D_z)_R u_R(t),$$

with

$$(C_z)_R = \begin{bmatrix} (C_y)_R \\ 0_{2 \times 4} \end{bmatrix}, \quad (D_z)_R = 0.5623 \times 10^{-7} \begin{bmatrix} 0_{2 \times 2} \\ I_{2 \times 2} \end{bmatrix},$$

to independently compute the gain matrix G_R . Arranging G_L and G_R in a block diagonal gain matrix, the following decentralized controller results

$$G_{dd} = 10^6 \times$$

$$\begin{bmatrix} 0.050 & -0.774 & -0.003 & -0.953 & -0.096 & -1.095 & 0 & 0 & 0 & 0 \\ 0.212 & -0.953 & -0.019 & -1.868 & -0.133 & -2.048 & 0 & 0 & 0 & 0 \\ 0.279 & -1.095 & 0.074 & -2.048 & -0.190 & -2.822 & 0 & 0 & 0 & 0 \\ 0 & 0 & 0 & 0 & 0 & 0 & 0.097 & -1.905 & -0.188 & -2.421 \\ 0 & 0 & 0 & 0 & 0 & 0 & 0.418 & -2.421 & -0.298 & -4.326 \end{bmatrix}$$

In this case, the minimum γ value is not available; however, the H_∞ norm can be directly computed using (21)–(23), resulting

$$\|T_{zw}(G_{dd})\|_\infty = 0.1550.$$

6.3 Numerical simulations

The maximum absolute inter-story drifts, and the maximum absolute control forces for the left and right building are displayed in Fig. 14 and Fig. 15, respectively. The full-scale El Centro 1940 earthquake has been taken as seismic excitation. Five cases of response are showed: (i) free response of the uncoupled system (denoted by Free in the legend), no passive or active control devices are working in this case; (ii) free response of the coupled system, i.e. response under passive control (denoted by Passive); (iii) response of the coupled system under the centralized active control (denoted by G_c); (iv) response of the coupled system under the decentralized active controller with centralized design (denoted by G_{dc}); and (v) response of the coupled system under the decentralized active controller with decentralized design (denoted by G_{dd}). The graphics show that a remarkable reduction

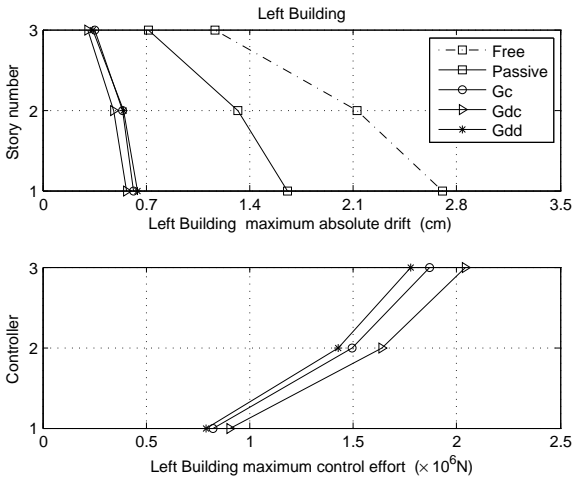


Fig. 14. Left building inter-story drifts and control forces

of the vibrational response is achieved by the passive control system. Regarding the active controllers, the performance of the decentralized controllers G_{dc} and G_{dd} is certainly excellent: both controllers behave practically the same as the overall centralized controller, in some cases with a slightly higher control effort.

Next, we consider the partial and full failure of the active decentralized controller G_{dd} . Table 1 presents the maximum inter-story drifts for full failure (Passive) and two cases of partial failure (Left failure, Right failure). The corresponding maximum absolute control actions are collected in Table 2. As a reference, these tables also

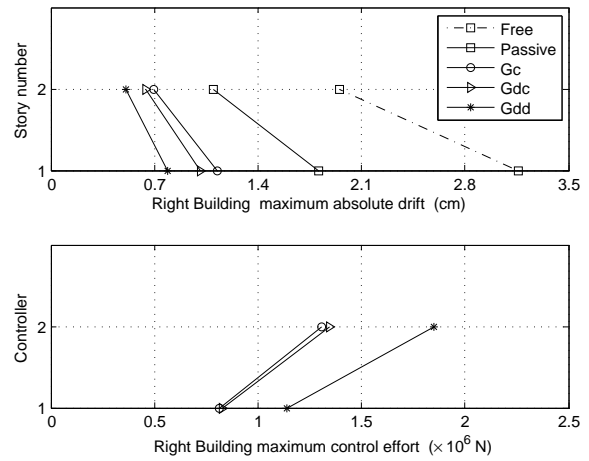


Fig. 15. Right building inter-story drifts and control forces

include the data for the free response, actively controlled response with the centralized controller G_c , and non-failure response with the decentralized controller G_{dd} .

	Left Building			Right Building	
	$y_1^{(l)}$	$y_2^{(l)}$	$y_3^{(l)}$	$y_1^{(r)}$	$y_2^{(r)}$
Free	2.71	2.13	1.17	3.16	1.95
Passive	1.65	1.32	0.72	1.81	1.10
Centralized (G_c)	0.62	0.54	0.35	1.13	0.70
Decentralized (G_{dd})	0.64	0.54	0.34	0.79	0.51
Left failure	1.24	1.04	0.61	0.83	0.53
Right failure	0.67	0.57	0.35	1.65	1.03

TABLE 1
Maximum absolute inter-story drifts (cm.)

In case of a full failure of the active control system, a remarkable reduction of the maximum inter-story drifts in both buildings is achieved by the passive element. When one of the local active controllers fails, the building that remains actively controlled is not affected by the failure. Moreover, the control forces in the working active controller increase slightly and act through the linking element to drive the response of the failing building to a level that is clearly below the level obtained by the pure passive control. In all the cases, the results achieved by the decentralized controller G_{dd} are similar to those obtained by the centralized control.

	Left Building			Right Building	
	$u_1^{(l)}$	$u_2^{(l)}$	$u_3^{(l)}$	$u_1^{(r)}$	$u_2^{(r)}$
Centralized (G_c)	0.82	1.49	1.87	0.81	1.31
Decentralized (G_{dd})	0.79	1.43	1.78	1.14	1.85
Left failure	0	0	0	1.19	1.93
Right failure	0.82	1.47	1.84	0	0

TABLE 2
Maximum absolute actuation force ($\times 10^6$ N)

The obtained results can also be seen from another interesting perspective. Buildings containing all sort of delicate equipment such as laboratories, operating rooms, large computer servers, telecommunication machinery, etc., may require a higher seismic protection than building containing more ordinary facilities as offices or meeting rooms. In this context, the four working states of the active decentralized controller: full working, left disabled, right disabled, and full disabled, can be understood as different control configurations corresponding to different levels of seismic protection. Thus, for two adjacent buildings which require a normal seismic protection, a passive link may be a good option; in the case that just one of the buildings needs special seismic protection, the data in Tables 1 and 2 suggest that the implementation of an active control system in this building together with a passive link may be an excellent option to obtain a proper level of seismic protection in both buildings. Moreover, the passive linking will help to mitigate pounding effects, and may also guarantee a remarkable level of seismic protection if the active control fails.

All computations have been performed using the Matlab LMI Control Toolbox [10].

CONCLUSIONS

An overview of some recent developments made by the authors in the field of vibrational control of structural systems, subject to seismic excitations, has been presented. Two categories of structural systems have been considered: (i) high-rise buildings, and (ii) multi-building systems. In the case of high-rise buildings, a mathematical framework given by the inclusion principle has been used to design semi-decentralized state-feedback controllers and output-feedback controllers. In the case of multi-building systems, a passive-active control strategy consisting in a combination of passive linking elements with a decentralized active control system has been developed. By means of three different building models, numerical simulations have showed that a remarkable reduction in the vibrational response is obtained following the proposed control strategies.

ACKNOWLEDGMENT

This work was supported in part by the Spanish Committee for Science and Technology (CICYT) under Grants DPI2008-06699-C02-02 and DPI2008-06564-C02-02.

REFERENCES

- [1] S.A. Anagnostopoulos. Building pounding re-examined: How serious a problem is it? In *Eleventh World Conference of Earthquake Engineering*, number Paper No 2108. Elsevier Science Ltd, 1996.
- [2] L. Bakule, J. Rodellar, and J.M. Rossell. Generalized selection of complementary matrices in the inclusion principle. *IEEE Transactions on Automatic Control*, 45(6):1237–1243, 2000.
- [3] L. Bakule, J. Rodellar, and J.M. Rossell. Structure of expansion-contraction matrices in the inclusion principle for dynamic systems. *SIAM J. Matrix Anal. Appl.*, 21(4):1136–1155, 2000.
- [4] S.D. Bharti, S.M. Dumne, and M.K. Shrimali. Seismic response analysis of adjacent buildings connected with magnetorheological dampers. *Engineering Structures*, (32):2122–2133, 2010.
- [5] A.V. Bhaskararao and R.S. Jangid. Seismic response of adjacent buildings connected with friction dampers. *Bulletin of Earthquake Engineering*, 4:43–64, 2006.
- [6] S. Boyd, L. El Ghaoui, E. Feron, and V. Balakrishnan. *Linear Matrix Inequalities in System and Control Theory*. SIAM Studies in Applied Mathematics, Philadelphia, USA, 1994.
- [7] X.-B. Chen and S.S. Stanković. Decomposition and decentralized control of systems with multi-overlapping structure. *Automatica*, 41:1765–1772, 2005.
- [8] R.E. Christenson, B.F. Spencer, and E.A. Johnson. Semiactive connected control method for adjacent multidegree-of-freedom buildings. *Journal of Engineering Mechanics*, 133(3):290–298, 2007.
- [9] G.P. Cimellaro. Coupled buildings control. In *Proceedings of the 16th ASCE Engineering Mechanics Conference*, University of Washington, Seattle, USA, 2003.
- [10] P. Gahinet, A. Nemirovski, A. Laub, and M. Chilali. *The LMI Control Toolbox*. The MathWorks, Inc., 1995.
- [11] A. İftar and Ü. Özgüner. Contractible controller design and optimal control with state and input inclusion. *Automatica*, 26(3):593–597, 1990.
- [12] M. Ikeda and D.D. Šiljak. Overlapping decentralized control with input, state, and output inclusion. *Control-Theory and Advanced Technology*, 2(2):155–172, 1986.
- [13] A.A. Liolios and A.K. Boglou. Chaotic behaviour in the non-linear optimal control of unilaterally contacting building systems during earthquakes. *Chaos, Solitons and Fractals*, 17:493–498, 2003.
- [14] V.A. Matsagar and R.S. Jangid. Viscoelastic damper connected to adjacent structures involving seismic isolation. *Journal of Civil Engineering and Management*, XI(4):309–322, 2005.
- [15] Y.Q. Ni and J.M. Ko. Random seismic response analysis of adjacent buildings coupled with non-linear hysteretic dampers. *Journal of Sound and Vibration*, 246(3):403–417, 2001.
- [16] F. Palacios-Quinonero, G. Pujol, J. Rodellar, and J.M. Rossell. Optimal complementary matrices in systems with overlapping decomposition: A computational approach. In *Proceedings of the 45th IEEE Conference on Decision and Control*, pages 253–257, San Diego, CA, USA, 2006.
- [17] F. Palacios-Quinonero, J. Rodellar, and J.M. Rossell. Sequential design of multi-overlapping controllers for longitudinal multi-overlapping systems. *Journal of Applied Mathematics and Computation*, 217(3):1170–1183, 2010.
- [18] F. Palacios-Quinonero, J. Rodellar, and J.M. Rossell. A design procedure for overlapped guaranteed cost controllers. In *Proceedings of the 17th IFAC World Congress*, pages 8701–8706, Seoul, Korea, July, 2008.
- [19] F. Palacios-Quinonero and J.M. Rossell. Decentralized control with information structure constraints. In *Proceedings of the 15th. International Workshop on Dynamics and Control*, pages 111–118, Tossa de Mar, Girona, Spain, 2009.
- [20] A. Preumont and K. Seto. *Active Control of Structures*. Wiley, United Kingdom, 2008.
- [21] J.M. Rossell and F. Palacios-Quinonero. Design of guaranteed cost overlapping controllers for a class of uncertain state-delay systems. In *Proceedings of the 2009 American Control Conference (ACC)*, pages 391–393, St. Louis, Missouri, USA, 2009.
- [22] J.M. Rossell, F. Palacios-Quinonero, and N. Luo. A contribution to the contractibility problem for overlapping controllers. In *Proceedings of the 12th. Large Scale Systems: Theory and Applications*, Villeneuve d’Ascq, Lille, France, July 11-14, 2010 2010.
- [23] J.M. Rossell, F. Palacios-Quinonero, and J. Rodellar. Semi-decentralized output feedback H_∞ control strategy for large building structures. In *Proceedings of the 5th. World Conference on Structural Control and Monitoring*, Shinjuku, Tokyo, July 12-14, 2010 2010.
- [24] S.S. Stanković and D.D. Šiljak. Contractibility of overlapping decentralized control. *Systems & Control Letters*, 44:189–199, 2001.
- [25] J. Teng and H. Liu. Optimum design of the control devices for adjacent structures under earthquake excitation. In *Proceedings of the 13th Mediterranean Conference on Control and Automation*, pages 328–333, Limassol, Cyprus, 2005.
- [26] D.D. Šiljak. *Decentralized Control of Complex Systems*. Academic Press, New York, USA, 1991.

$$\begin{aligned}
 K_c^{(a)} &= 10^7 \times \begin{bmatrix} -0.1466 & -2.8886 & 0 & -0.0048 & 0 & -0.0032 & 0 & -0.0016 \\ 0 & -0.0048 & -0.1466 & -2.8870 & 0 & -0.0032 & 0 & -0.0016 \\ 0 & -0.0032 & 0 & -0.0032 & -0.1466 & -2.8854 & 0 & -0.0016 \\ 0 & -0.0016 & 0 & -0.0016 & 0 & -0.0016 & -0.1466 & -2.8838 \end{bmatrix} \\
 K_c^{(b)} &= 10^7 \times \begin{bmatrix} 0.1457 & 2.4536 & -0.0009 & -1.2934 & -0.0006 & -0.3237 & -0.0003 & -0.1065 \\ 0.1447 & 1.1602 & 0.1450 & 2.1298 & -0.0012 & -1.3998 & -0.0006 & -0.3237 \\ 0.1441 & 0.8365 & 0.1444 & 1.0537 & 0.1450 & 2.1298 & -0.0009 & -1.2934 \\ 0.1438 & 0.7300 & 0.1441 & 0.8365 & 0.1447 & 1.1602 & 0.1457 & 2.4536 \end{bmatrix} \\
 \tilde{K}_1^{(3)} = K_o^{(a)} &= 10^7 \times \begin{bmatrix} -0.1466 & -2.8854 & 0 & -0.0016 & 0 & 0 & 0 & 0 \\ 0 & -0.0008 & -0.1466 & -2.8835 & 0 & -0.0003 & 0 & 0 \\ 0 & 0 & 0 & -0.0003 & -0.1466 & -2.8833 & 0 & -0.0003 \\ 0 & 0 & 0 & 0 & 0 & -0.0005 & -0.1466 & -2.8833 \end{bmatrix} \\
 K_o^{(b)} &= 10^7 \times \begin{bmatrix} 0.1463 & 2.5551 & -0.0003 & -1.1441 & 0 & 0 & 0 & 0 \\ 0.0730 & 0.7055 & 1.3720 & 2.3862 & 1.4215 & -0.6378 & 0 & 0 \\ 0 & 0 & -2.8050 & 0.6207 & 2.6785 & 2.3672 & 1.4215 & -0.6378 \\ 0 & 0 & 0 & 0 & -5.6100 & 1.2415 & 2.7594 & 2.5171 \end{bmatrix} \\
 K_{\text{full}} &= 10^8 \times \begin{bmatrix} 3.0628 & -0.4736 & -0.7680 & -0.4051 & -1.8408 & -0.3356 & -1.8081 & -0.2429 & -0.9725 & -0.1251 \\ 4.1829 & -0.7172 & -0.4061 & -0.6365 & -2.9673 & -0.5129 & -2.6692 & -0.3709 & -1.4004 & -0.1908 \\ 5.3852 & -0.8895 & -0.8618 & -0.8027 & -2.9653 & -0.6592 & -3.4503 & -0.4727 & -1.6801 & -0.2414 \\ 6.1557 & -1.0033 & -0.9786 & -0.9098 & -3.6438 & -0.7536 & -3.1788 & -0.5381 & -2.1621 & -0.2755 \\ 6.8456 & -1.0655 & -0.8928 & -0.9806 & -3.8938 & -0.8277 & -3.6532 & -0.5908 & -1.6983 & -0.3048 \end{bmatrix} \\
 K_{\text{part}} &= 10^8 \times \begin{bmatrix} -1.5837 & -0.4251 & 1.8711 & -0.7768 & -0.1777 & 0.4861 & 0.1253 \\ -2.1535 & -0.4317 & 3.4493 & -2.7004 & -0.1992 & 1.3583 & 0.0080 \\ 3.1188 & -0.6564 & -3.0014 & -0.1039 & -0.5116 & -0.0218 & -0.0940 \\ 2.2077 & -0.5904 & -0.9987 & -2.1916 & -0.4793 & 1.0541 & -0.0561 \\ 1.3499 & -0.6501 & 1.0673 & -4.4912 & -0.5289 & 2.2303 & -0.0038 \end{bmatrix} \\
 K_{\text{over}} &= 10^8 \times \begin{bmatrix} -0.0840 & -0.2155 & -0.2747 & 0.7047 & -0.0384 & 0 & 0 \\ -0.6488 & -0.2121 & 1.3000 & -1.2768 & -0.0541 & 0 & 0 \\ 0.3615 & -0.1325 & -0.1151 & 0.3146 & -0.5292 & -0.4684 & 0.0827 \\ 0 & 0 & 0 & -0.6961 & -0.9064 & 0.2657 & -0.2638 \\ 0 & 0 & 0 & -1.5700 & -0.9095 & 1.2155 & 0.0057 \end{bmatrix} \\
 \dots \\
 A &= 10^3 \times \begin{bmatrix} 0 & 0.0010 & 0 & 0 & 0 & 0 & 0 & 0 & 0 & 0 \\ -0.9850 & -0.0085 & 0.9850 & 0.0085 & 0 & 0 & 0 & 0 & 0 & 0 \\ 0 & 0 & 0 & 0.0010 & 0 & 0 & 0 & 0 & 0 & 0 \\ 0.9850 & 0.0085 & -1.9699 & -0.0170 & 0.9850 & 0.0085 & 0 & 0 & 0 & 0 \\ 0 & 0 & 0 & 0 & 0 & 0.0010 & 0 & 0 & 0 & 0 \\ 0 & 0 & 0.9850 & 0.0085 & -1.9699 & -0.0170 & 0.9850 & 0.0085 & 0 & 0 \\ 0 & 0 & 0 & 0 & 0 & 0 & 0 & 0.0010 & 0 & 0 \\ 0 & 0 & 0 & 0 & 0.9850 & 0.0085 & -1.9699 & -0.0170 & 0.9850 & 0.0085 \\ 0 & 0 & 0 & 0 & 0 & 0 & 0 & 0 & 0 & 0.0010 \\ 0 & 0 & 0 & 0 & 0 & 0 & 0.9850 & 0.0085 & -1.9699 & -0.0170 \end{bmatrix} \\
 B &= 10^{-5} \times \begin{bmatrix} 0 & 0 & 0 & 0 & 0 \\ 0.2894 & 0 & 0 & 0 & 0 \\ 0 & 0 & 0 & 0 & 0 \\ -0.2894 & 0.2894 & 0 & 0 & 0 \\ 0 & 0 & 0 & 0 & 0 \\ 0 & -0.2894 & 0.2894 & 0 & 0 \\ 0 & 0 & 0 & 0 & 0 \\ 0 & 0 & -0.2894 & 0.2894 & 0 \\ 0 & 0 & 0 & 0 & 0 \\ 0 & 0 & 0 & -0.2894 & 0.2894 \end{bmatrix} \\
 E &= [0, -1, 0, 0, 0, 0, 0, 0, 0, 0]^T
 \end{aligned}$$

Fig. 16. Gain matrices for different kinds of controllers / Matrices of the five-story building model.

[27] Y. Wang, J.P. Lynch, and K.H. Law. Decentralized H_∞ controller design for large-scale civil structures. *Earthquake Engineering and Structural Dynamics*, 38:377–401, 2009.

[28] Z. Yang, Y.L. Xu, and X.L. Lu. Experimental seismic study of adjacent buildings with fluid dampers. *Journal of Structural Engineering*, 129(2):197–205, 2003.

[29] Z.G. Ying, Y.Q. Ni, and J.M. Ko. Stochastic optimal coupling-control of adjacent building structures. *Computers and Structures*, 81:2775–2787, 2003.

[30] A.I. Zečević and D.D. Šiljak. Design of robust static output feedback for large-scale systems. *IEEE Transactions on Automatic Control*, 49(11):2040–2044, 2004.

[31] W.S. Zhang and Y.L. Xu. Dynamic characteristics and seismic response of adjacent buildings linked by discrete dampers. *Earthquake Engineering and Structural Dynamics*, 28:1163–1185, 1999.